Ecology

Synthetic Eco-Evolutionary Dynamics in Simple Molecular Environment

Luca Casiraghi, Francesco Mambretti, Anna Tovo, Elvezia Maria Paraboschi, Samir Suweis, Tommaso Bellini

Dipartimento di Biotecnologie Mediche e Medicina Traslazionale, Università degli Studi di Milano, Via Fratelli Cervi, 93 - L.I.T.A., Segrate, 20054, Italy • Dipartimento di Fisica e Astronomia, Università degli Studi di Padova, Via Marzolo 8, Padova, 35131, Italy • Department of Biomedical Sciences, Humanitas University, Via Rita Levi Montalcini 4, Pieve Emanuele, 20072, Italy • IRCCS, Humanitas Clinical and Research Center, Via Manzoni 56, Rozzano, 20089, Italy

Reviewed Preprint

Revised by authors after peer review.

About eLife's process

Reviewed preprint version 2
February 13, 2024 (this version)

Reviewed preprint version 1
September 12, 2023

Posted to preprint server
July 25, 2023

Sent for peer review
June 29, 2023

Abstract

The understanding of eco-evolutionary dynamics, and in particular the mechanism of coexistence of species, is still fragmentary and in need of test bench model systems. To this aim we developed a variant of SELEX in-vitro selection to study the evolution of a population of $\sim 10^{15}$ single-strand DNA oligonucleotide 'individuals'. We begin with a seed of random sequences which we select via affinity capture from $\sim 10^{12}$ DNA oligomers of fixed sequence ('resources') over which they compete. At each cycle ('generation'), the ecosystem is replenished via PCR amplification of survivors. Massive parallel sequencing indicates that across generations the variety of sequences ('species') drastically decreases, while some of them become populous and dominate the ecosystem. The simplicity of our approach, in which survival is granted by hybridization, enables a quantitative investigation of fitness through a statistical analysis of binding energies. We find that the strength of individual-resource binding dominates the selection in the first generations, while inter and intra-individual interactions become important in later stages, in parallel with the emergence of prototypical forms of mutualism and parasitism.

eLife assessment

In this **important** study, the authors develop a promising experimental approach to a central question in ecology: What are the contributions of resource use and interactions in the shaping of an ecosystem? For this, they develop a synthetic ecosystem set-up, a variant of SELEX that allows very detailed control over ecological variables. The evidence is **convincing**, and the work should be of broad interest to the ecology community, leading to further quantitative studies.

Introduction

A central effort in theoretical biology and ecology is to provide an effective description of the intimate, but often subtle, relationship between a given environment and the evolution of its ecosystem. In the case of simple environments without geographical isolation and physical barriers, as the one here considered, the emergence of species and phenotyping clustering ***Davis (1943)***; ***Rundle and Nosil (2005)***; ***Keymer et al. (2012)***; ***Gupta et al. (2021***) is generally considered an outcome of the competition for the limited available resources ***Dieckmann and Doebeli (1999)***; ***Pigolotti et al. (2007)***; ***de Aguiar et al. (2009)***; ***Anceschi et al. (2018***). The coexistence of stable species is ecologically understood in terms of "niches", indicating the unique role and position that a particular species occupies within an ecosystem. According to the "niche hypothesis" ***Chase and Leibold (2009)***; ***Peterson (2011)***; ***Anceschi et al. (2018***), biodiversity is limited by the number of "niches" (or types of resources) that are present since no two species can occupy the same niche indefinitely, as one would eventually out-compete the other ***Levin (1970)***; ***Gupta et al. (2021***).

Fitness, which quantifies species reproductive success and thus also their relationship with the environment ***De Visser and Krug (2014***), cannot generally be defined in a predictive way even in the most idealized systems ***Thurner et al. (2010)***; ***Wiser and Lenski (2015***). Indeed, despite the efforts to identify simple case study systems, the evolution of populations formed by a variety of species remains difficult to model and to quantitatively characterize because of the inherent complexity of ecosystems and living beings, of the large number of potentially relevant variables of difficult access, and of the role of stochasticity ***Catalán et al. (2017***).

In this scenario, introducing new tools to explore and test eco-evolutionary models, concepts and interpretations appear as the best strategy toward new understanding ***Solé (2016***). Along this line, various synthetic biological platforms have been proposed in the last years ***Ichihashi et al. (2013)***; ***Tizei et al. (2016)***; ***Parrilla-Gutierrez et al. (2017)***; ***Kauffman et al. (2018)***; ***Adamala and Szostak (2013)***; ***Katla et al. (2023***) that exploit different principles and mechanisms, and focused on *in-vivo*, *in-vitro*, *ex-vivo*, or *in-silico* approaches. For example, in ***Ichihashi et al. (2013***) a "cell-like" model system is proposed, in which the evolution of one long genomic RNA (> 2,000 nt-long) was investigated in detail under the action of a selective pressure ultimately provided by its biological meaning. Despite the tremendous simplification provided by this approach, the constructed artificial cell is still a complex system that includes ribosomes, lipids, translation factors, accessory proteins, tRNAs and amino acids. While most of the synthetic biological platforms are based on the establishment of cell-like, compartmentalized systems involving complex biomolecular milieus and processes ***Tizei et al. (2016***), a few are devoted to investigate, with distinct strategies, the competition between two coexisting vescicle-based species competing for resources (vescicle-forming molecules) in a non-biochemical context ***Adamala and Szostak (2013)***; ***Katla et al. (2023***). These articles demonstrate that typical evolution concepts, such as competition or resources and niche exclusion principle, can be applied to "non-biological" systems.

We here propose a synthetic eco-evolutionary scheme, with no cell-like compartmentalization and no connection to the molecular biology of the cell: no coding sequences, no translation, no proteins involved. We consider an ecosystem formed by a large crowd ($\sim 10^{15}$) of distinct molecular individuals interacting with each other and competing for survival in an environment with fixed resources, and we focus on the process by which selection and competition drive the emergence of dominating species. Specifically, we study the evolution of a pool of 50-base-long single strand DNA oligomers with random sequences, a choice that ensures that in the initial solution each molecule is unique. The mechanisms of survival and mutual interactions are based on DNA hybridization. By exploiting the wealth of tools and knowledge about DNA code selective pairing and DNA synthesis, amplification and sequencing, we create a condition in which a limited number of

accessible and computable variables controls the destiny of an ecosystem formed by biological molecules that evolve in a non-biological way, i.e. with no reference to the biological meaning of their sequence.

The results of our work, demonstrating the intimate connection between fitness and ecological interactions, belong to the growing body of studies ***Fussmann et al. (2007)***; ***Vetsigian (2017)***; ***Camacho Mateu et al. (2021***) showing that ecological and evolutionary processes are strictly related in the emergence and maintenance of species.

Results

Affinity-based DNA Synthetic Evolution

We introduce here a variant of SELEX for in-vitro synthetic evolution of oligonucleotides to develop protein-binding aptamers ***Ellington and Szostak (1990)***; ***Tuerk and Gold (1990***). In standard SELEX protocol, the evolving oligonucleotides are selected at each cycle by their interactions of with the target protein. In the experiment here reported, we implemented a selective mechanism based on the affinity capture provided by magnetic beads carrying single-stranded DNA (ssDNA) filaments of fixed length $L = 20$ and sequence, that act as targets (or resources, **Figure 1a**). Selection is thus primarily based on the sequence of the DNA individuals and its level of complementarity to the targets. This marks a significant difference with SELEX, in which the aptamer-protein interaction depends instead on higher order factors such as the secondary structure of the oligonucleotides and the variety of binding sites on the folded protein. Being these hard to model, predict and control, SELEX has never been considered, to the best of our knowledge, as a useful experimental test bench to understand evolution.

In our Affinity-based DNA Synthetic Evolution (ADSE) protocol, evolution starts from an initial pool of DNA Individuals (DNAi), chosen to be of fixed length $L = 50$ and random sequence. Each sequence indicates a 'species'. Since the potential molecular variety is $4^{50} \sim 10^{30}$ while our experiments use about 10^{15} initial molecules, each species in the initial pool has only one DNAi. The following evolution process is sketched in **Figure 1b**, Figure 1-figure supplement 2, and is given by three steps.

1. *Selection*: the seed population is mixed with a given amount of dispersed capture beads. After a suitable incubation time, the beads are extracted from the solution and the bound oligomers released and saved. The rest of the original solution is discarded;
2. *Amplification*: the pool of "survived" oligomers is PCR amplified about 1000 times to recover the initial molarity;
3. *Sequencing*: a small portion of the amplified sample (1-3 10^6 molecules) is analyzed by massive parallel sequencing (MPS). These molecules are thus removed from the evolving pool.

These steps constitute a cycle - one generation of evolution - that we repeated up to 24 times in two independent evolution histories, which we refer to as "Oligo 1" and "Oligo 2". In the following, we present in detail the results of the Oligo 1 evolution, while Oligo 2 results are described in the figure supplements.

In actuality, to enable amplification and sequencing, DNAi are built by flanking the 50mer with two 25 base long fixed sequences that enable primer binding for a total length of 100 bases. Such two terminal segments of the DNAi are made inactive during selection by hybridization with oligomers of perfect complementarity, as sketched in **Figure 1a**, Figure 1-figure supplement 1.

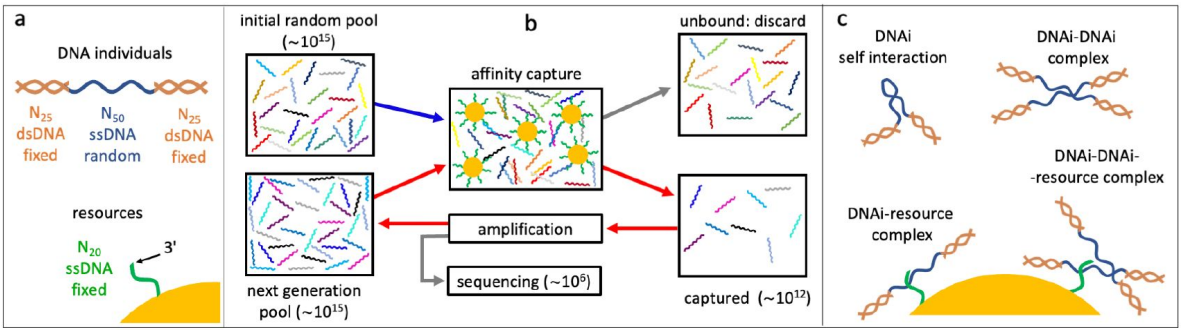

Figure 1.

Affinity-based DNA Synthetic Evolution (ADSE). a: structure of the DNA oligomers participating in ADSE as individuals (DNAi) and target resources. b: steps in the ADSE. The process starts with a random-sequence DNAi population. The capture by magnetic bead-conjugated resources provides the selection: bead-bound DNAi are amplified to form the new generation, a small fraction of which is sequenced by massive parallel sequencing. The rest of the original solution is discarded. Red arrows mark the steps of each ADSE cycle. c: possible interaction motifs involving DNAi.

The online version of this article includes the following figure supplements:

Figure 1-figure supplement 1 Detailed structure of DNA individuals.

Figure 1-figure supplement 2 Detailed scheme of the Affinity-based DNA Synthetic Evolution protocol.

A key feature of ADSE is that DNAi can interact not only with the resources, but also with itself and with each other, and also potentially form complexes binding to the affinity beads as summarized in **Figure 1c**. Indeed, the choice of a length of 50 for the DNAi interaction was thought to enable - in principle - simultaneous resource and mutual binding.

PCR amplification can be of high fidelity or error-prone, the latter choice enabling genetic drift and, potentially, speciation. Since our primary goal was to first investigate fitness in a pool of competing species within a given niche, defined in our case by the 20 base long resources, we opted for a high-fidelity amplification, and left the investigation of high mutations regimes to a follow- up experiment. Because of the many PCR cycles required in the ADSE scheme, the amplification inevitably leads to the formation of artifacts in the form of longer sequences ***Tolle et al. (2014***), a phenomenon that intrinsically sets a limit to the number of generations that can be explored (see Appendix 1).

As detailed below, the ADSE protocol enables observing a non-trivial evolution of the DNAi ecosystem across generations, the emergence of dominating species and non-monotonic population evolution. It also enables to appreciate the role of inter-specific interactions and their contribution to fitness.

Evolution of the DNAi ecosystem

The main output of the synthetic evolution that we are proposing is the dataset $\{\text{DNAi}\}_j$ obtained by sequencing DNAi at the various cycles ($1 \le j \le 24$ being the index of the cycle). We find that the initial random ecosystem markedly changes with ADSE generations as shown in **Figure 2a**, in which we have plotted the evolution of: (i) the fraction F_D of the total population formed by distinct nucleotide sequences (red dots). F_D drops from 1 to nearly 0, indicating that initially DNAi are all different from each other, while after 24 generations the number of distinct sequences is much smaller than the number of DNAi. This indicates that most of the initial sequences become progressively "extinct"; (ii) The fraction F_{10} of the total population formed by the 10 most abundant DNA sequences (black dots). F_{10} is initially close to 0 - being each sequence represented by a single DNAi, and grows to about 25% at cycle 12 and 55% at cycle 24 - indicating that the offspring of 10 initial "mother" sequences becomes the majority of the system. This loss of diversity can also be quantified by the zipped file size of the list of sequences ***Benedetto et al. (2002***) or by computing its Shannon entropy ***Hill (1973***), both markedly decreasing during evolution (see Appendix 1).

Since in ADSE survival depends on bead capture, we expect DNAi-resource binding strength to be an essential ingredient of fitness. To this aim we compute the mean DNAi-resources binding free energy ΔG_{DR} across generations, plotted in **Figure 2b** (blue squares, right-hand side y- axis). Specifically, ΔG_{DR} has been computed based on DNAi and resource sequences by using the standard "nearest-neighbor approximation" for the thermodynamics of DNA hybridization ***SantaLucia Jr (1998); Ghosh et al. (2019); Plata et al. (2021***), as implemented in the NUPACK tool in Python ***Zadeh et al. (2011***). Being this computation of some complexity, we could perform it only on batches of 1000 DNAi randomly chosen within $\{\text{DNAi}\}_j$, the error bars expressing the uncertainty introduced by such down-sampling (see Material and Methods section). For reference, a DNA 20mer perfectly complementary to the resource would bind to it with an energy of approximately -24 *kcal/mol*.

To perform a faster - and thus more complete - analysis of the resource-binding energy in the evolving population, we have introduced ω, a simpler quantifier than ΔG_{DR}. ω is the length of the longest consecutive number of bases within each DNAi that is complementary to the resource sequence (considering all possible relative positions of the two), in which we allow for single pairing errors and 1-base bulges ***Mambretti et al. (2022a***). ω ignores factors that are relevant for the free energy, such as the specificity of the sequence and the fraction of CG pairs, and thus is inadequate to evaluate the binding strength of specific DNAi. However, its average value $\langle\omega\rangle$

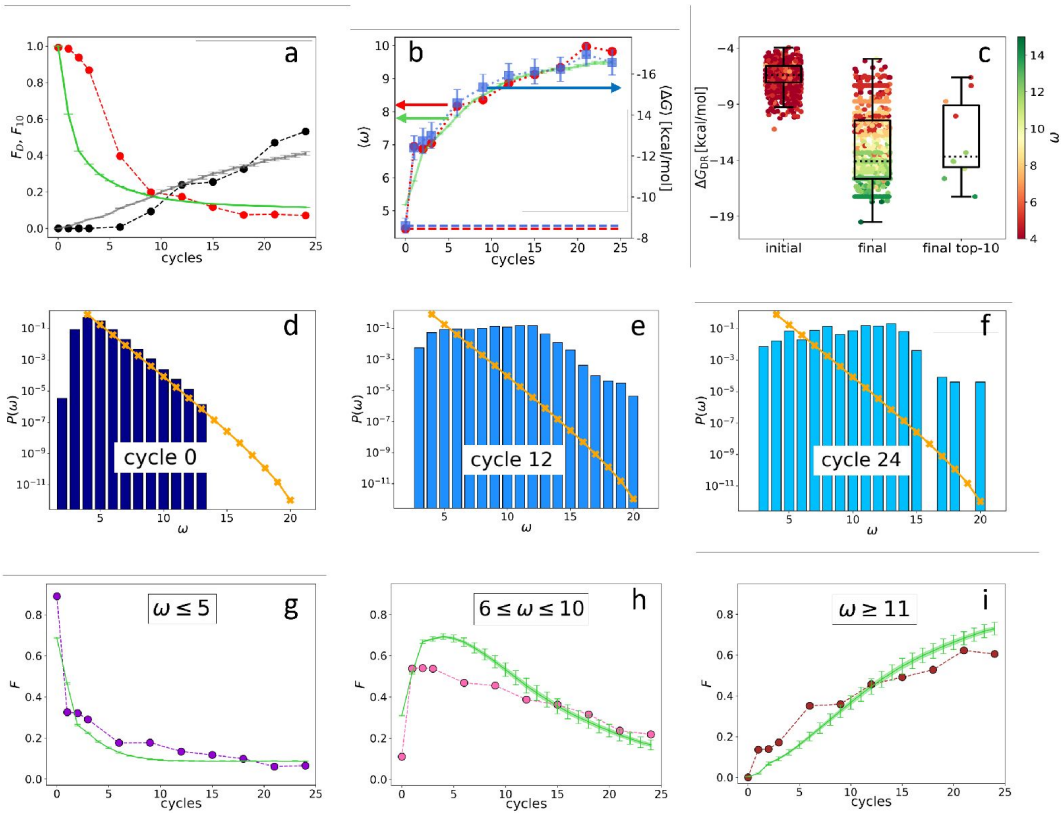

Figure 2.

Evolution of the DNAi population (Oligo1 data). Time is expressed in ADSE cycles. a: fraction F_D of the total population formed by different sequences obtained from the experiment (red dots) and computed with the IBEE model (green line), fraction F_{10} of the total population formed by the 10 most abundant sequences (experimental: black dots, IBEE model: gray line). b: $\langle\omega\rangle$ computed on the whole population in each generation (red dots, left-hand side y-axis); $\langle\Delta G_{DR}\rangle$ computed on a sample of 1000 randomly chosen DNAi from the population in each generation (blue dots, right-hand side y-axis); data fitting with the IBEE model (green line, left-hand side y-axis). The left and right y axes were scaled so that $\langle\Delta G_{DR}\rangle$ and $\langle\omega\rangle$ computed on a pool of random sequence DNAi would coincide (dashed blue and red lines, respectively). c: boxplots and scatterplots of $\langle\Delta G_{DR}\rangle$ in ensembles of 1000 random sequences (left), 1000 randomly chosen DNAi extracted from the experimental population at cycle 24 (middle) and from the top-10 most populous DNAi at the same cycle (right). The color code is assigned to each point based on its ω value (color bar). d-f: probability distributions p (ω) for cycles 0 (d), 12 (e) and 24 (f). In the latter histogram, empty bins result from sub-sampling. Orange points and lines are the distributions evaluated with the null model. g-i: evolution of the abundance (expressed as fraction of the total population F) of sequences whose ω is small ($3 \le \omega \le 5$- panel g), medium ($6 \le \omega \le 10$ - panel h) and large ($11 \le \omega$ - panel i) as obtained from the experiments (dots) and with the IBEE model (green lines). The model results are averages over 20 simulations. The online version of this article includes the following figure supplements:

Figure 2-figure supplement 1. Time evolution of the fraction of PCR by-products and of their $\langle\omega\rangle$.

Figure 2-figure supplement 2. Probability distributions p ($\langle\omega\rangle$)of PCR by-products at cycles 0 and 24.

Figure 2-figure supplement 3. Sequencing technical replicate.

Figure 2-figure supplement 4. Checking PCR effects on DNAi selection.

Figure 2-figure supplement 5. Time evolution of $\langle\omega\rangle$ for the Oligo2.

Figure 2-figure supplement 6. Probability distributions p ($\langle\omega\rangle$)at cycles 0 and 18 for the Oligo2.

Figure 2-figure supplement 7. Experimental vs IBEE time evolution of the population zip ratio and of the Shannon Entropy associated to the RSA distribution.

Figure 2-figure supplement 8. Experimental vs IBEE $\langle\omega\rangle$ time evolution, for two different IBEE hyperparameters choices.

Figure 2-figure supplement 9. Experimental vs IBEE $\langle\omega\rangle$time evolution, for different sizes and compositions of the starting population of IBEE model.

computed for the entire population in each generation (**Figure 2b**, red dots, left-hand side y-axis) grows almost identically to$\langle \Delta G_{DR} \rangle$ (blue dots, right-hand side y-axis). The $\langle \omega \rangle$ axis has been scaled so that its value (computed on a pool of random sequence DNAi - dashed red line) matches, in the plot, $\langle \Delta G_{DR} \rangle$ (computed on the same pool - dashed blue line). A more detailed comparison between ω and ΔG_{DR} is given in **Figure 2c**, showing box plots with ΔG_{DR} on the y axis and ω expressed through color code. Both are computed from a random selection of 1000 distinct DNAi from the initial (left hand side box), the final populations (central box), and the top 10 most frequent sequences in the final generation (right hand side box). The result further strengthens the validity, in our statistical context, of ω as a quantifier of the strength of interaction with the resources ***Mambretti et al. (2022a)***.

Figure 2b shows that, during ADSE, $\langle \omega \rangle$ tends to saturate at a value $\omega_{sat} \approx 10$, indicating that no relevant selective advantage is gained when $\omega > 10$, in agreement with the notion that the residence time of hybridized oligomers becomes larger than typical experimental times when $\omega > 12$ ***Di Leo et al. (2022***).

Figure 2d-f describes the evolution of the ecosystem $\{\text{DNAi}\}_j$ by showing $p\ (\omega)$, the fraction of DNAi having overlap ω with the resource evaluated in the initial pool (panel d) and at generation 12 (e) and 24 (f). $p\ (\omega)$ clearly evolves, its small ω components being progressively lost, while individuals with large ω grow in number, as they are more successful in being selected and amplified. It might be worth pointing out that the appearance of non-zero $p\ (\omega > 13)$ at generation 12, while $p\ (\omega > 13) = 0$ in the initial distribution, is an effect of the under-sampling involved in the sequencing procedure.

The different destiny of DNAi with distinct ω values is shown in **Figure 2g-i**, where we show the temporal (i.e. across generation) evolution of the fraction of the total population whose ω is in the following ranges: $3 \le \omega \le 5$ (panel g), $6 \le \omega \le 10$ (panel h) and $11 \le \omega$ (panel i). As expected, DNAi with weak affinity to the resources decrease, while those with large affinity increase. Interestingly, DNAi with intermediate affinity exhibit a non-monotonic behavior, indicating that the conditions for survival change during the evolution, reflecting the evolution of the ecosystem.

Null Model and Eco-evolutionary Algorithm

In order to better understand the experimental outcomes, we build first a null random model without evolution and then an Individual-Based Eco-Evolutionary (IBEE) model enabling predictions for $p\ (\omega)$.

The null model describes the interaction between individuals in the initial pool $\{\text{DNAi}_{j=0}\}$ of random sequences and the resources within a purely combinatorial framework (see Methods and Appendix 3 for mathematical details). In this model, we attach a random string of length 50 to the resource string in a random position, and we compute the maximum consecutive overlap, accepting the binding only if it is at least formed by 3 complementary basis.

The resulting analytical $p_0(\omega)$, plotted in **Figure 2d** (orange crosses) closely matches the data obtained from sequencing, confirming the random-sequence nature of $\{\text{DNAi}\}_{j=0}\}$. The analytical $p_0(\omega)$ extends to a ω range where no data are available due to the limited size of the sequenced pool. The comparison between $p_0(\omega)$ and $p\ (\omega)$ in panels e and f shows that the exponential decay of $p_0(\omega)$ at large ω is maintained even in generation 12 and partly in generation 24, further supporting the notion that the selective advantage of ω saturates at large ω.

In the IBEE algorithm we consider N_p individuals. Each has a fitness $f_i(\omega)$ ($i = 1, 2, .., N_p$) that depends on its affinity ω with the resource. At time $t = 0$ we assign ω to each individual based on $p_0(\omega)$ from the null model. Then, for each evolutive cycle, we model competition and selection so that out of N_p individuals, only N_r survives. This is attained as a combination of two processes: a fraction x of the N_r sequences results from sampling individuals from the N_p population, each with

a survival probability $f(\omega) \in (0, 1)$ (selection); the remaining fraction $1 - x$ is extracted completely from the N_p individuals. The latter group is meant to mimic "neutral drift" (as it would be expressed in evolutionary language) provided by non-specific binding to the beads. The N_r survivers are amplified by identical copying back to N_p, the starting population of the next evolutionary cycle (the introduction of very rare mutations do not affect the results). We perform 24 evolutionary cycles.

As expected, the outcome of the eco-evolutionary dynamics strongly depends on the shape of the fitness function. We model it as:

$$f(\omega) = \left(\frac{\omega^*}{\omega_{max}} \right)^{\gamma}$$

where ω_{max} is the (cycle-dependent) largest value of ω within the actual population and, $\omega^* = \omega$ if $\omega < \omega_{sat}$, while $\omega^* = \omega_{sat}$ otherwise. ω_{sat} and γ are parameters to be tuned in the comparison with the observed $\langle\omega\rangle$. ω_{sat} expresses the loss of fitness gain for $\omega > \omega_{sat}$ yielding the saturation of $\langle\omega\rangle$. γ represents the strength with which $f\langle\omega\rangle$depends on ω, and thus the rate at which low ω individuals are discarded. γ may of course depend on time on account of the evolving ecosystem.

After grid search we find $x = 0.9$, indicating that the random drift contributes to about 10% of survival at each cycle, and $\omega_{th} = 10$, in agreement with the observations prompted by the saturating behavior of $\langle\omega\rangle$. We also find that the data cannot be approximated with a single value of γ, as visible in Figure 2-figure supplement 8. Data can instead be very well matched assuming $\gamma = 3$ for the first 5 cycles and $\gamma = 1$ for the remaining cycles, as shown in **Figure 2b**, green line. With the same choice of parameters, the IBEE fitness based model captures the decrease in the diversity of the DNAi ecosystem (**Figure 2a**, green and grey lines) and the temporal (i.e. across generations) evolution of the relative population abundance of DNAi in the three ω intervals in **Figure 2**, panels **g, h** and **i**.

The effect of the system size and initial conditions on the IBEE results, discussed in the Appendix 2, do not qualitatively change the models results. Error-bars on simulations have been obtained by averaging 20 independent runs, starting from the same initial conditions. As can be observed, the variability among simulations is negligible.

Also, the IBEE model with a fixed γ would respect the increasing, decreasing, and non-monotonic trends of the data in **Figure 2**, but not quantitatively. The change in γ, and thus in fitness, is indeed necessary to reproduce the observed$\langle\omega\rangle$with the IBEE model. This is a key result of our investigation because it indicates that, even in simple conditions of ADSE environment (fixed resource and low mutation rate), survival is controlled by more than affinity to the resources, as discussed in the analysis below.

Self and mutual DNAi interactions are evolutionary drivers

While ω is certainly a key driver of the observed evolution, it is clearly not the only one. The fact that the top 10 most represented sequences become, in the last cycle, about 55% of the total population (**Figure 2a**) implies that, even among sequences with large ω, only a tiny minority come to dominate, while the largest part of them eventually disappear. Moreover, the 10 most represented sequences do not stand out for their particularly large ΔG_{DR} or ω, as noticeable in **Figure 2c**. The same data are plotted in **Figure 3a** as a p (ΔG_{DR}) distribution to enable comparing the free energy distribution in the initial population (purple shading), in the final population (blue columns), and in the top 10 (black columns). These elements support the notion that survival and dominance must also be due to factors in addition to ω, which we thus explored.

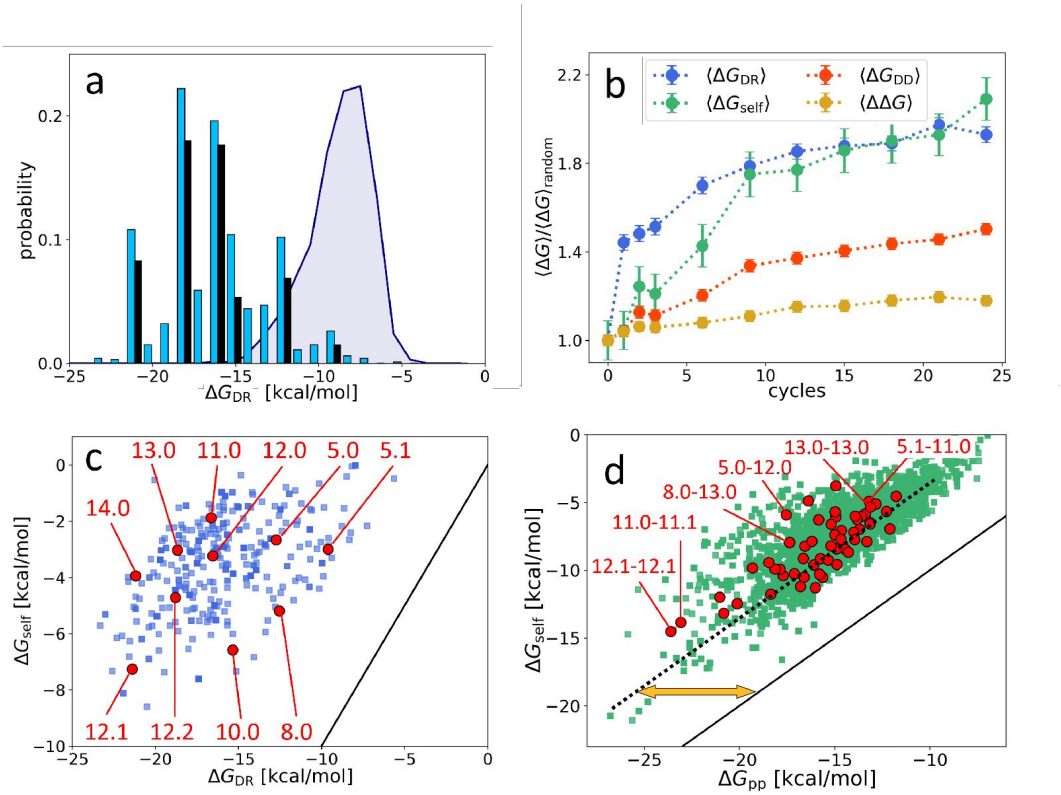

Figure 3.

Distribution and evolution of free energy quantifiers (Oligo1 data). a: probability distribution for the DNAi-resource binding free energy computed by NUPACK, $p(\Delta G_{DR})$, for the initial population (grey shading), for the final population (random choice of 1000 DNAi - cyan columns, top 10 most populous sequences - black columns). b: time evolution, expressed in cycles, for various mean free energies $\langle \Delta G \rangle$, normalized to their value computed on pools of random sequences. All ΔG are computed by NUPACK on sets of 1000 individuals: $\langle \Delta G_{DR} \rangle$ (blue dots); unimolecular self-interaction $\langle \Delta G_{self} \rangle$ (green dots); bimolecular mutual DNAi interaction $\langle \Delta G_{DD} \rangle$ (red dots); mutual, self-subtracted interaction $\langle \Delta\Delta G \rangle$ (yellow dots). c: scatter plot of ΔG_{self} vs. ΔG_{DR} computed for 1000 DNAi in the final population (blue squares). Red dots mark the point relative to the 10 most populous sequences, as identified by the labels. Note that the x-axis scale of panels a and c is the same, enabling identifying sequences. d: scatter plot computed on 10^4 DNAi pairs from the final population comparing $\Delta G_{self,j} + \Delta G_{self,l}$ and $\Delta G_{DD,kl}$ (green squares). Red dots mark the pair formed by the 10 most populous sequences, some of which identified by labels. With respect to the condition $\Delta G_{DD,kl} = \Delta G_{self,j} + \Delta G_{self,l}$ (black line), data are on average displaced by $\Delta\Delta G \sim 7.5$ kcal/mol (yellow arrow). The online version of this article includes the following figure supplements:

Figure 3-figure supplement 1. Three examples of different relative positions for sequence-sequence attachment.

Figure 3-figure supplement 2. Scheme of target-DNAi interaction, from a combinatorial standpoint.

Figure 3-figure supplement 3. Null model without threshold, analytical and simulated, with an even and uneven nucleotides distribution.

Figure 3-figure supplement 4. Null model with/without threshold, simulated and analytical.

Figure 3b shows the value, across the 24 generations, of two other contributions to the total free energy, normalized to their value computed in random sequences, so to enable comparing their relative variations: $\langle \Delta G_{\text{self}} \rangle$ (green symbols), the average unimolecular free energy, expressing the average strength of the internal folding of each DNAi; $\langle \Delta G_{DD} \rangle$ (red dots), the total bimolecular DNAi-DNAi free energy, comprising both self and mutual interactions. For comparison, we also plot the normalized value of $\langle \Delta G_{DR} \rangle$ (blue dots). As for the case of $\langle \Delta G_{DR} \rangle$, $\langle \Delta G_{\text{self}} \rangle$ and $\langle \Delta G_{DD} \rangle$ are computed by randomly selecting 1000 individuals or pairs, respectively, from the population at cycle j and using the NUPACK tool to compute the values.

Figure 3b reveals that $\langle \Delta G_{\text{self}} \rangle$ grows in time even more than $\langle \Delta G_{DR} \rangle$, but with a different progression: ΔG_{DR} grows faster in the first cycles to later saturate, while the growth of $\langle \Delta G_{\text{self}} \rangle$ is more uniform.

Since $\langle \Delta G_{DR} \rangle$ is computed as the free energy of the whole DNAi-resource structure, it includes contributions of self energy associated to hairpins in the DNAi. Thus the growth of $\langle \Delta G_{DR} \rangle$ could actually depend on the growth in $\langle \Delta G_{\text{self}} \rangle$ (but not the contrary). To investigate this possibility, **Figure 3c** displays the scatter plot between $\langle \Delta G_{DR} \rangle$ and$\langle \Delta G_{\text{self}} \rangle$, for a randomly chosen subset of DNAi at $j = 24$. In evidence are the 10 points corresponding to the 10 most populous sequences. The plot shows weak or no correlation, and a relevant shift with respect to $\langle \Delta G_{\text{self}} \rangle = \langle \Delta G_{DR} \rangle$ (black line), demonstrating negligible dependence of $\langle \Delta G_{DR} \rangle$ on $\langle \Delta G_{\text{self}} \rangle$ and indicating that these two quantities reflect two independent driving forces in the ADSE selection mechanism. The existence of two different growth regimes suggests that in the first stages of ADSE the selection is mainly dominated by affinity with the resources, while in later generations the requirement of stronger unimolecular folding becomes more important.

A similar scatter plot analysis for $\langle \Delta G_{DD} \rangle$ yields a different outcome. **Figure 3 d** compares the $\langle \Delta G_{DD} \rangle$ computed for two selected DNAi (individual “k” and “l”) and the sum of ΔG_{self} of the same two DNAi. The apparent correlation indicates that, *on average*, a large part of ΔG_{DD} simply embodies the growth of self-energy, although the difference $\Delta\Delta G \equiv \Delta G_{DD,kl} - \Delta G_{\text{self},k} - \Delta G_{\text{self},l}$ (orange arrow) is non-negligible. **Figure 3b** shows the behavior of $\langle \Delta\Delta G \rangle$ across cycles (orange squares). Despite the resulting mild growth of $\Delta\Delta G$ might appear not relevant, it actually indicated that ADSE, independently of ω, selects strings that have higher reciprocal affinity than a random DNAi set (see Appendix 2). Indeed, the selection process could instead have promoted a decrease of the same quantity. It should be noted that mutual interactions might also involve the unfolding of hairpins self-structures, in which case their strength is much larger than $\Delta\Delta G$.

Self-interactions and mutual interactions can compete with the binding of DNAi to the resources either when they involve the same nucleobases or through steric hindrance. Therefore, we could expect that the increase of ΔG_{DR} would lead to a decrease of both ΔG_{self} and ΔG_{DD}. Their unforeseen growth in the ADSE process is hence an indication of the selective advantage they convey. We interpret this behavior as an indirect sign that mutual DNAi interactions, more than just an impediment, are major deadly threats for their survival. To avoid them, DNAi need screening. Indeed, the strong growth of self-interactions, and the mild increment in mutual interactions, could represent the emergence of “defensive” strategies, as discussed below.

In our search for evolution quantifiers other than resource binding strength, we also found that selection favors binding to resource sequences close to their resource 3’ terminal, away from the bead surface (see Figure 4-figure supplement 2). While this is expected, being that terminal less constrained and in a less crowded environment, it also provides useful clues to further analysis.

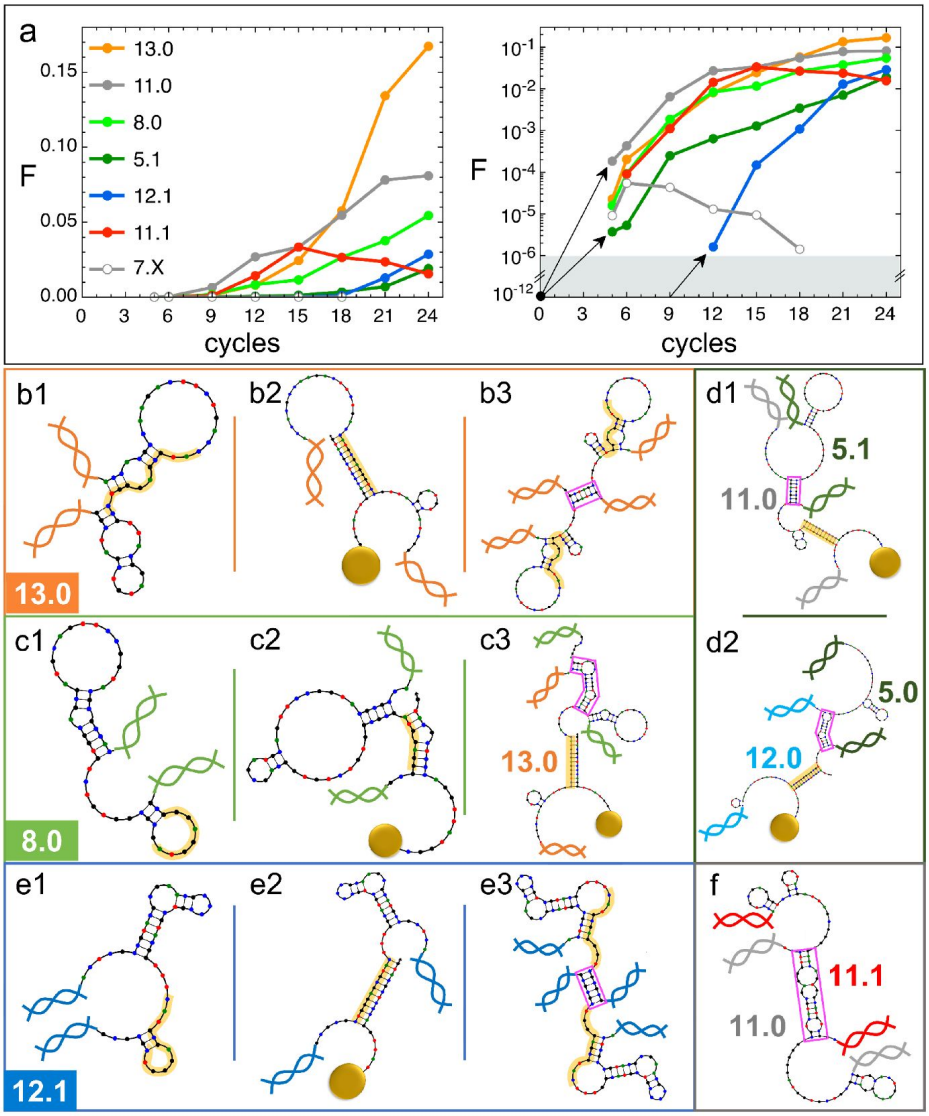

Figure 4.

Natural history of DNAi species (Oligo1 data). a: fraction *F* of {DNAi} that belong to a choice of specific species as a function of the ADSE cycles, in linear (left) and logarithmic (right) scale. Arrows connect the initial condition (one individual per species at cycle 0) to the earliest detection via sequencing, across the 6 order of magnitudes gap (grey shading). The same growth is assumed for species 12.1, suggesting its appearance by mutation occurred at generation 9. b-f: self-interactions (b1, c1, e1), resource interactions (b2, c2, e2, d1, d2) and mutual interactions (b3, c3, e3, d1, d2, f) of selected species, sketched as per the NUPACK output. Nucleobases color coded (G - black, C - blue, A - green, T - red). Paired bases are connected. Double and single stand regions are represented as straight and curved lines, respectively. As in **Figure 1a**, terminal blocks of DNAi are marked as graphic double helices colored according to the legend of panel a, and beads as sketched yellow spheres. Yellow shading: section of DNAi complementary to resources. Pink frames: regions of hybridization between DNAi. b: interactions involving species 13.0 including its homodimerization (b3). c: interactions involving species 8.0, including its binding to 13.0 (c3). e: interactions involving species 12.1, including its homodimerization (e3). d and f: DNAi heterodimers interactions suggesting parasitism (d1), and possibly mutualism (d2) and mutual damage (f).

The online version of this article includes the following figure supplements:

Figure 4-figure supplement 1. Evolution of the intra-species interaction strengths ($\langle \Delta G_{pp} \rangle$).

Figure 4-figure supplement 2. 2D probability for selected DNAi, shown at different experimental cycles, to have a given $\langle \omega \rangle$ jointly with a given attachment coordinate to a target strand.

The evolution of DNAi species

We examined the evolution of DNAi species, i.e. the change in numerosity of the groups of DNAi having equal sequence, which we report in **Figure 4a** relative to a limited set of (mainly) successful species (for a larger selection see SI). Data in **Figure 4a** are expressed as the fraction F of the total population that belong to a given species. It can be noticed that species that are later becoming dominant "appear" in our analysis only at generation 5 in a single or a few copies. This is reasonable since we sequence a sample of $\sim 10^6$ DNAi over the much larger population of $\sim 10^{12}$ survived individuals.

Species are named after their ω value, combined with an index (e.g. "12.0", "12.1", "12.2" ...) expressing their ranking in populousness. In **Figure 3**, panels **c** and **d**, we marked and labeled in red the free energy values associated to the 10 species dominating in the last generation and labeled the corresponding species or pairs of species. It can be noticed that the dominant species are not - as one could naively expect - at the extremes of the energies distributions and assigned, confirming that the statistical trends do not enable, by themselves, a full understanding of ADSE.

The populousness of ADSE species does not have standard patterns of evolution. This is true even when limiting the observation to the successful species in **Figure 4a** whose population growths are varied and do not reflect in any simple way the energy quantifiers. Conversely, species with similar energy quantifiers may have opposite fate, either becoming dominant or rapidly extinguishing or else displaying a non-monotonic population evolution. It is worth pointing out that all species start equal, each represented in the original pool by a single molecule, which on this scale would appear as a $F \approx 10^{-12}$ (black dot in **Figure 4a**, right panel).

We thus decided to seek further understanding on the survival of the fittest in ADSE by inspecting the "natural history" of a few species (see Tables 2, 3 in the Supplementary Information).

13.0 and 11.0 (orange and gray dots in **Figure 4a**) are, respectively, the most and second most populous species in the last generation. It might be relevant to mention that the replica of ADSE described in the SI leads to different dominant sequences, as expected on the basis of the distinct initial pool and on the key role of randomness and sampling in the first cycles. At generation 24, 13.0 and 11.0 have grown to more than 85% and 53% of DNAi with $\omega = 13$ and $\omega = 11$, respectively. 13.0, and 11.0 likewise, have a weak self-interaction (**Figure 3c**), corresponding to hairpins that provide a mild defense to mutual interactions, as schematically sketched in **Figure 4**, panel b1. The hairpins involve most of the bases that are complementary to the resource (yellow shading), leaving however a few unpaired bases that might act as toehold to initiate resource binding. The resource binding takes place at its 3' terminus (panel b2). A bit puzzled about the success of these two species we also explored their capacity of mutual interactions and found that both of them are capable of forming homodimers, as shown in panel b3 for 13.0 (binding energy marked in **Figure 3d**). Such dimers can bind resources at both ends (yellow shading regions), giving 13.0 and 11.0 self-screening and divalent binding capacity. We argue this to be a crucial drive toward success of these two species, which also explains why their growth has such an increment in the latest generations, following the probability of dimer formation.

The third most populous sequence (species 8.0) is characterized by a weak resource interaction which includes a bulge (see **Figure 3c**). While its survival rationale appears clear - good defensive self-binding (panel c1) and interaction targeting the 3' end of the resource (panel c2) - it is hard to accept this could be the cause of the success. Again, inspecting the mutual interaction we found that 8.0 efficiently interacts with 13.0 (as marked in **Figure 3d**), in a region (frame in pink) that does not conflict with the capacity of 13.0 to bind the resource (panel c3). We speculate that this parasitic capacity of 8.0 adds to the weak intrinsic binding to lead to a remarkable success of this species.

As a test to this concept, we focus on species 5.1, whose binding strength to the resource is the weakest in the top 10 species and one of the weakest among all the survivors of generation 24 (**Figure 3c**), a feature that questions its success. However, by inspecting mutual interactions, we find its binding to 11.0 to be strong and stable (pink frame in panel d1 and **Figure 4d1**). An analogous behavior is found for species 5.0 and its interaction to 12.0 (panel d2), confirming that parasitism is an emerging successful survival solution in ADSE.

We then inspect 12.1 since it has largest ΔG_{DR} and ΔG_{self} among the top 10 species (**Figure 3c**). Species 12.1 has all the features to succeed in ADSE: it forms a weak hairpin with the bases involved in the binding with the resources and a strong hairpin that protects the rest of the ssDNA segment (panel e1); it strongly binds to the resource with the bond ending at its 3' terminal (panel e2); it forms homodimers capable of double resource binding, analogous to that of 13.0 (panel e3). Remarkably, 12.1 emerges only late in ADSE (**Figure 4a**, blue dots), a very unusual behavior when compared to the other many species we have considered. The combination of this late appearance and of the remarkable growth in F afterward suggests that 12.1 is the outcome of one of the rare *mutations* that can occur even with the high quality PCR that we adopted. By assuming an initial growth analogous to that of dominant species (black arrows in panel a), we argue that such mutation occurred around generation 9, where we have found ancestors having sequence equal to 12.1 except for 4 bases.

F has a monotonic increase for most of the species that become dominant in the latest generations. This behavior is however not at all general. Non-monotonic F, growing during in the first generations and decreasing to extinction afterward, is the general behavior for the majority of species that do not become extinct in the first cycle, as also shown - through their average behavior - in **Figure 2h**. An examples of these is species 7.X (empty dots in **Figures 4a** and **4b**).

More intriguing is when a non-monotonic behavior is observed for one of the dominating species. This is the case of 11.1, whose growth can be again attributed to an effective screening and a good binding to the resources, but whose decrease is harder to justify. To understand it we again investigate mutual interactions, and we find a strong 11.0-11.1 bond (sketched in panel f), which, differently from the DNAi-DNAi complex examined above, competes with resource binding. We thus speculate that the fall of 11.1 is a consequence of the rise of 11.0, which has become frequent enough to make the formation of the complex 11.0-11.1 probable, which lowers the survival probability of both species. This could also explain why species 11.0 has such an irregular growth pattern, with a slowing down when 11.1 becomes highly populated.

The insight gained by these case-studies enables appreciating how self and mutual interactions can affect the fate of species in ADSE beyond what we could discern through distributions and average quantifiers. Indeed, this analysis shows that the success of the dominant ASDE species can be achieved through different combinations of resource and mutual DNAi interactions, a fact that makes the evolution of population so varied and generation dependent and explains why, in the latest generations of ADSE, the population distribution $p(\Delta G)$ (**Figure 3a**) is so irregular.

Discussion and Conclusion

We have here introduced ADSE, a synthetic molecular evolution protocol that exploits sequencing technology and DNA interaction computability to provide a test-bed for key concepts in ecology and evolution. Although the simple scheme of ADSE enables to perform studies in which mutations and resource drifts can be introduced, we performed experiments by adopting the most simple environment within this protocol, *i.e.* by holding fixed the capture sequence and

minimizing mutations. This choice was aimed at achieving a condition dominated by competition and selection, which enables investigating the nature of fitness in this simplified evolution process.

Our experiments and their comparison with theoretical models indicate that fitness is not a simple function of the direct competitive advantage of strong binding to the resources, as it could have been naively expected. Resource binding is indeed the dominant factor in the first part of the evolution (cycles 1-5), producing a fast growth of $\langle\omega\rangle$ *compatib*le with a strong dependence of the survival probability on ω ($f \propto \omega^3$). However, as $\langle\omega\rangle$reaches a value corresponding to bonds of *moderate* stability ***Woodside et al. (2006***) - approximately from generation 6 onward - the selective pressure related to resource binding decreases ($f \propto \omega$), a condition enabling to appreciate other factors at play. Which are these factors is suggested by the different growth patterns of ΔG_{DR} and ΔG_{self}, the former dominating the first cycles while the latter drives the later stages. However, the quantification of binding energies is not sufficient to predict the fate of individual species, that also depends on interaction details (location of binding and hairpins, secondary structures) and possibly on kinetics.

In fact, by design, DNAi can interact with themselves, both internally - forming hairpin-like structures - and mutually - leading to the formation of complexes. These interactions can either coexist when they involve non-overlapping sequences - or they can become competitive. Our experiments reveal that, among the wide variety of conditions made available by the initial random seed, ADSE generally promotes those that combine a good interaction with the resources and a structure capable of screening from mutual DNAi interactions conflicting with binding to the beads. By exploring hybridisation-dependent DNAi secondary structures - the only ones accessible with simple analytical tools, we found three basic motifs: hairpins due to self-interactions (as for species 12.1), formation of DNAi homoduplets (as for species 13.0 and 11.0), and formation of dimers of DNAi belonging to distinct species. The latter can bring to distinct prototypical behavior: it can be the basis of *parasitism*, as in the case of the pairs 8.0-13.0 and 5.1-11.0, it can lead to *extinction* with no benefit for either species (as in the case of 15.0-12.0), or it can provide - at least in principle *mutualism*. While we do not have a solid proof, clues suggest that cooperation might be active in the case of the interaction between species 5.0 and 12.0, since 12.0 has a weak self-defensive system and since the populations of 12.0 and 5.0 evolve very similarly (see Table 2). Finally, we cannot exclude a possible role of the formation of multi-DNAi multivalent complexes. This is the case of species 12.0 and 15.0 whose pattern of multivalent mutual interactions can, in principle, allow higher order interactions (see Appendix 2).

Fitness in ADSE is the outcome of a complex interplay of all these elements. The history of single species in **Figure 4** indicates that the nature of fitness is beyond what can be captured by analyzing the probability distributions of the relevant parameters describing structure and interactions. Moreover, the variety of population evolution patterns enlightens the fundamental fact that despite the constancy of resources, the progressive modification of the ecosystem brings about a change in the competition modes, and thus in fitness. A forthcoming work focused on a limited number of species will be devoted to better disentangle the nature of fitness in ADSE.

The evolution of the ADSE ecosystem, which corresponds to a marked decrement of its entropy with 2/3 of the initial species become extinct in the first 5 generations - and potentially terminating with the indication of a single winner species leads instead, in the last cycles, to a significant number of dominant species all still growing at the expense of subservient ones, indicating that in their direct competition none of them is strongly prevailing despite - or maybe thanks to - their distinct survival strategies and their very different population share. Hence, while the niche hypothesis could still be verified in the long run - beyond the experimental limitations due to PCR - it is clear that its drive is weak, suggesting that it could be overcome by environmental fluctuations, thus allowing for coexistence of different species even in a single niche environment.

Methods

Our experimental design takes advantage of a selective capture mechanism where magnetic beads carrying single-stranded DNA filaments of fixed length and sequence (resources) target DNA individuals (DNAi) (Figure 1-figure supplement 1) present in a DNA library based on their level of complementarity. This process of selection is carried out through subsequent steps that are described in detail in the next paragraphs and represented in Figure 1-figure supplement 2.

Library design

The DNA library contains 100-nt-long sequences where a randomized central region of 50 nucleotides is flanked by 25-nt-long fixed sequences at both its 5' and 3' ends. The fixed regions provide an anchor point for primer annealing, required to perform PCR reactions during the amplification phase (see below). These terminal segments are made inactive by hybridization with oligomers of perfect complementarity (blockers), so that they are not involved in the selection phase. The blockers, as well as the fixed regions of the DNA library, have been designed to avoid hybridization with the resources. In addition, the blockers carry a phosphate group at their 3' end to prevent them from functioning as primers during the PCR amplification. Following the above described criteria, we designed two sets of sequences (Table 1 in the Supplementary Information), called Oligo1 (whose results are presented in the main text) and Oligo2 that was used as a replication experiment. All the oligonucleotides used in this work were purchased from Integrated DNA Technologies, Coralville, IA, USA (Table 1).

Beads preparation

The capture of DNAi within the DNA library was performed with carboxylic acid magnetic beads (M-270 Dynabeads, Invitrogen, Carlsbad, CA) coated with the resources. The resources are 20-nucleotide-long, 5'-amino-modified oligonucleotides. Their coupling to the beads surface was performed according to the manufacturer's instructions. Following the activation and coupling procedure, the beads were washed in Tris-HCl (50mM, pH 7.4), and stored in the same buffer in single-use aliquotes.

Sample preparation

The starting samples were prepared in 1X SSC buffer (0.15M sodium chloride, 15mM sodium citrate, pH 7.0). In detail, the Oligo1 (or Oligo2) library (0.75nmol) was mixed with the blockers (2.25nmol) in 1:3 molar ratio to saturate all the available interaction sites between the blockers and the fixed regions of the DNA library. The sample was then denatured at 95°C for 5 minutes, then slowly brought to room temperature using a thermal cycler (MasterCycler Nexus Gradient, Eppendorf, Hamburg, Germany).

Selection phase

The beads, coupled with the resources, are mixed with the sample, prepared as described above. The capture of the DNAi is carried out at 40°C for 2 hours in stirring (600rpm, ThermoMixer, Eppendorf). Once the selection phase is completed, the sample is incubated for 2 minutes on a magnet and the supernatant is removed. The beads, that are now bound to the captured DNAi, are washed three times in SSC 1X buffer to eliminate the aspecific sequences. Finally, the beads are resuspended in water and incubated for 5 minutes at 60°C to recover the DNAi from the resources. The sample is quickly placed on the magnet and after 2 minutes the supernatant containing the selected DNAi is collected and then quantified by NanoDrop (Thermofisher Scientific).

Control experiments were performed showing that no artifact in ADSE are introduced in ADSE because of non-specific interactions with the magnetic beads (see Appendix 1, Experimental controls).

Amplification phase

The captured DNAi are then amplified by PCR with Q5® Hot Start High-Fidelity DNA Polymerase (New England Biolabs, Ipswich, MA, USA). DNA samples were diluted 10 times and 3µl were used for each PCR reaction. The PCR was performed in a final volume of 25µL using 0.25µL of polymerase, and each primer had a final primer concentration of 2.5µM. To allow the regeneration of the single strand library, the reverse primer was designed to carry a 5' biotin modification (see next paragraph for details). The thermal protocol was the following: i) denaturation step at 98 ° C for 2 minutes, ii) 28 cycles characterized by three thermal steps: 10 seconds at 98°C, 10 seconds at 68°C for Oligo1 (69°C for Oligo2) and 1 second at 72°C, iii) 2 minutes at 72°C. The annealing temperature was kept higher than conventional protocols to endure that hairpins or DNAi dimers are melted. For each generation, 10 different PCR reactions were performed. The PCR products were then checked for size on a 2% TBE 1X agarose gel.

Control experiments were performed showing that no artifact are introduced in ADSE from the amplification steps (see Appendix 1, Experimental controls).

Regeneration phase

PCR products were purified by precipitation with 2.5 volumes of ethanol and 0.1 volumes of sodium acetate 2M, pH 5.2. After an overnight precipitation at -20°C, the pellet was washed with ethanol 75%, resuspended in water and quantified using the Qubit fluorometer (Invitrogen, Waltham, MA, USA). The single-strand regeneration was performed with streptavidin-coated magnetic beads (M- 270 Dynabeads, Invitrogen, Carlsbad, CA) according to manufacturer's instructions. Briefly, the PCR product was incubated for 15 minutes on a rotator with the magnetic beads. After 2 washes with binding and washing buffer (10mM Tris–HCl pH 7.5, 1mM EDTA, 0.2M NaCl) and a third one with SSC 1X buffer, an alkaline denaturation was performed by incubating the beads with 150mM NaOH for 10 minutes to induce the separation of the two DNA strands. This way it is possible to recover the unlabeled DNA strand in solution. The ssDNA is then collected and buffered with 1.25M acetic acid and TE 1X. The regenerated ssDNA is ready for the next round of selection and amplification.

Sequencing of the recovered products

To check the growth of DNAi species in our experimental model, some generations were sequenced through next-generation sequencing techniques. To prepare the sample for sequencing, the DNAi species captured as described in the "Selection phase" paragraph were first PCR-amplified using the same conditions discussed before. However, in this case, both forward and reverse primers were unlabelled. After PCR purification, performed as already described (see "regeneration phase" paragraph), the products were quantified and used to obtain libraries. About 300ng of DNA were used as starting material for the NEBNext® Ultra™ II DNA Library Prep Kit for Illumina ® (New England Biolabs), and libraries were prepared following the manufacturer's instruction. Sequencing was performed with the NextSeq™ 550 sequencer (Illumina, San Diego, CA, USA) and a paired-end strategy to obtain 75-nt long reads.

A technical replica was performed to assess the fluctuations intrinsic to sequencing in the context of ADSE (see Appendix 1, Experimental controls)

Replicas

The experimental workflow was repeated on two different sets of DNA libraries: Oligo1, whose results are described in the main text, and Oligo2, used as a replicate. The experimental conditions and procedures were the same for both sets of oligonucleotides, the only differences being the sequences of the fixed parts of the DNA libraries (and hence of the blockers and primers) and of the resources (Table 1). As a consequence, also the PCR conditions had to be adjusted, in terms of the annealing temperature that is one degree higher for Oligo2.

Eco-Evolutionary algorithm

To support experimental observation with a simple abstract model, we developed an Evolutionary Algorithm where a population of N_p sequences evolves in presence of $N_r < N_p$ shorter sequences. In particular, N_r individuals in this population are selected at each cycle depending on their fitness, i.e. on their affinity to the resource, expressed via their ω with it. These survived sequences are then amplified by a factor of (roughly) N_p/N_r. In this work, two types of fitness functions have been explored: the first one is merely linearly proportional to the ω of each individual (i.e. $\frac{\omega}{\Sigma\omega}$, where $\Sigma\omega$ is the sum of the ω values of the whole population), while the other one is a modification of the previous fitness which sets it to be $\frac{\omega_{th}}{\Sigma\omega}$ beyond a threshold value ω_{th}. The code is written in C++, exploiting MPI ***Message Passing Interface Forum (2021)*** and Armadillo ***Sanderson and Curtin (2016***, 2018) libraries for acceleration.

NUPACK calculations

We resorted to NUPACK for nucleotide sequences analysis, for the prediction of their free energies at equilibrium, either alone or when binding to one or two other oligomers. Schemes like those shown in **Figure 4** have been obtained via the NUPACK web application ***Zadeh et al. (2011***), while massive ΔG calculations have been performed with custom Python codes exploiting NUPACK Python package (v4.0.0.27) ***Fornace et al. (2020)***; ***Dirks et al. (2007***). The model is dna04 and ensemble='some-nupack3'; $T = 40^{\circ}$C and $[Na^{+}] = 0.24$ M, as in the experiments. Concentration of each species in the tube has been arbitrarily set to 10^{-6} M. Detection of hairpins and other secondary structures has been performed visually (thanks to the oxView software ***Bohlin et al. (2022)***; ***Poppleton et al. (2020***)).

Acknowledgements

T.B. acknowledges support from MIUR-PRIN (Grant No. 2017Z55KCW). F.M. and S.S. acknowledge CloudVeneto (*http://cloudveneto.it*, ***Andreetto et al. (2019***)) for the use of computing and storage facilities, through the SEDES and HPC-Physics projects.

Conflict of interest

The authors declare no conflict of interest.

Availability of data and materials

The datasets generated and analysed during the current study are available from the corresponding author on reasonable request.

Code availability

The Jupyter Notebooks used for the present analysis are available at *https://github.com/francescomambretti/stat_phys_synthetic_biodiversity*.

Author Contributions

SS, EMP and TB conceived and designed the study; LC and EMP designed protocols and performed the experiments; FM, AT and SS analyzed the data and developed the theoretical models; LC and FM performed NUPACK analysis; LC, FM, SS and TB interpreted the data and wrote the manuscript.

Appendix 1 Data analysis protocol

Since we performed a paired-end sequencing, for each experimental cycle two FASTQ files were generated (R1 and R2).

The data shown in the paper all come from the cumulative analysis of R1 and R2 files. To analyze such files, we have developed an ad-hoc package (in Python and C++), currently maintained at *https://github.com/francescomambretti/stat_phys_synthetic_biodiversity*. Here follows a scheme of the main steps of the analysis:

1. Read FASTQ file, extracting the list of single-stranded DNA (ssDNA) sequences. Reverse sequences are reverted and complemented, so to have all the sequences oriented as $5' \to 3'$. Fixed sequences at the ends are removed in this way: if the full blocker is present, then the 50 bases after it are retained. If some of the last bases of the blocker are lost (it may happen), then just remove the primer and keep the subsequent 50 bases. Slightly different choices for this cut of the sequences turned out to be substantially irrelevant for all the results.
2. Each sequence can be either saved or discarded, according to some filtering procedure. Criteria include the minimum quality of the read (≥ 10, measured according to the *Phred* score), the minimum and maximum allowed length, the presence of invalid nucleotides (indicated by 'N' in the FASTQ file) and other checks (see below in particular for PCR by-products).
3. The 'survived' sequences are processed, computing the related observables. Unique sequences are identified and their degeneracy is computed. This allows to monitor the time evolution of the abundance of each species (where the equivalence: DNA sequence-species holds).
4. For each of these unique ssDNAs, we compute the indicators quantifying the 'affinity' with the target sequence: in particular, the maximum consecutive overlap (MCO) and eventually the binding free energy with the resource and/or other oligomers.
5. Several post-processing options are available, such as: generating histograms of the ssDNA population based on their affinity with the resource; tracking the time evolution of dominant strands; determining the fraction of the total population covered by the n most abundant strands. All these quantities can be plotted by suitable Python scripts, provided in the GitHub repository.

By-Product Formation from PCR Amplification

During the amplification phase, described in our workflow, we observed the formation of PCR by-products. This phenomenon is known in SELEX systems, especially when an oligonucleotide library characterized by high heterogeneity is PCR-amplified ***Tolle et al. (2014***). The generation of these by- products is caused by unspecific hybridization of the primers and/or of oligonucleotides, leading to PCR products abnormal in terms of length and distribution of random/fixed sequences. To limit this phenomenon we adopted blocker oligos with a phosphate group at 3', so that they do not act as primers, and a stringent PCR protocol, characterized by: i) a high annealing temperature, ii) fewer PCR cycles, iii) a high primer concentration, iv) a very short elongation step (1s). Moreover, during the data analysis step, we developed an algorithm to identify and remove these spurious sequences.

PCR by-products are identified among the sequenced oligomers according to the following criteria:

- if either the sequence (after the cut of the blocker as previously described) contains at least n consecutive bases identical to n of the $5'$ blocker (i.e. an n-long MCO with a subsequence of the Primer1-F)

- or it has at least n consecutive bases identical to n of the 3' blocker

then this sequence is considered as a by-product and excluded from the analysis.

Figure 2-figure supplement 1a shows how such unwanted sequences become ≈ 30% of the total sampled population at cycle 15 and then the striking majority (> 95%) in the last cycle, setting *de facto* an upper limit to the number of feasible experimental cycles. On the other hand, as we can see from Figure 2-figure supplement 1b, the behaviour of $\langle\omega\rangle$ *for the* by-products is very similar to the one observed considering only regular oligomers, therefore the one observed considering only re their presence does not affect the main outcome of the experiment.

In Figure 2-figure supplement 2 the p (ω) for the first and last cycle of only the by-products of Oligo 1 are displayed and compared with the null model prediction. The main evolutive trend is also present in these sequences, which have however been discarded from all the analyses.

Intrinsic limitations of the molecular approach

Possible biases in our workflow are intrinsic to both PCR and Illumina sequencing technologies (e.g. sequencing of homopolymers or amplification of GC-rich sequences). However, in our experimental procedure we implemented approaches and solutions to reduce them. Regarding PCR, we developed an optimized thermal protocol, characterized by very short denaturation, annealing and amplification steps performed at high temperatures. Regarding Illumina sequencing, we can't rule out a bias against specific sequences (e.g, homopolymers), which however should not be captured during the selection step, due to the design of the resource. Also, the libraries subjected to sequencing are characterized by a low complexity since, according to the experimental design, the first and last 25 nucleotides are the same for all DNAi. The complexity further decreases during cycles because of the decrease in DNAi diversity. This could constitute a problem, since in the design of Illumina instruments nucleotide diversity, especially in the first sequencing cycles, is critical for cluster filtering, optimal run performance and high-quality data generation. To overcome this limitation, the obtained libraries were run together with much larger and more complex and diverse library preparations (and as a consequence the number of reads we obtained was in the range of a few millions per run, a small fraction of the total).

Experimental controls

To check the specificity and the robustness of our approach, we implemented different control steps: i) a negative control with bare beads, ii) a technical replicate of the sequencing, iii) a PCR replica.

Negative control

First, we tested the effect of a possible non-specific binding of DNAi to the beads on the selection process. Beads were prepared as described in the Methods section, but they were not coated with the resources. The selection step was performed following the described protocol, and six selection cycles were carried out. We were able to recover DNAi after each selection steps, due to an non-specific binding between the beads surface and DNAi. After sequencing cycle 6, we compared the results with the corresponding cycles of the Oligo1 and Oligo2 experiments. The most abundant sequence in the negative control had a relative occurrence of 0.05%, whereas the dominant strand in the 6th generation in Oligo1 and Oligo2 had an abundance of 8% and 16%, respectively, i.e. 40-80 times larger. This indicates that the natural drift provoked by non-specific interactions with bare beads is more than one order of magnitude smaller than the selection induced by the affinity with the resource.

Technical replicate

Second, we tested the effect of sampling on the consistency of the sequencing results. Since only a small fraction of the recovered sample is actually analyzed, we sequenced twice the library derived from Oligo1 cycle 9, and we identified in both replicates the most abundant DNA species, defined as those with at least 100 sequencing reads (corresponding to 27.42% of the total reads). Among the 800 DNA species that satisfied this requirement, 93.6% are found in both replicates; the remaining ones are characterized by a low representation, close to 100 reads. Subsequently, we compared the abundance of DNAi populations between the two replicates (Figure 2-figure supplement 3), by calculating the ratio between the number of reads of each shared DNA species in each replicate, after normalizing for the total number of reads obtained from sequencing. We found an average ratio of 0.965 (standard deviation = 0.119), and we observed significant fluctuations only for the least populated species. Overall these results indicate that the effect of sampling (and thus the sequencing readout, as well as possible PCR amplification errors) don't have a significant impact on the selection process.

PCR effects on DNAi selection

Third, we tested the effect of PCR amplification on the selection process. Starting from Oligo1 cycle 9 sample, we performed an additional PCR amplification round (equal to those used to connect ADSE generations) and we proceeded directly to sequencing with no beads-selection step. We then compared the ensemble of oligos obtained in this way, which we named Oligo 1 "cycle 9 replica", with both the original Oligo1 cycle 9, and with Oligo1 cycle 10. We sampled 20 times 4 x 10^5 sequences from the cycle 9 dataset, from cycle 9 replica and from cycle 10 with a bootstrap approach. To compare the three systems we extracted the fraction of the population of each covered by the 10 most abundant individuals (Figure 2-figure supplement 4). We found that the 10 most abundant species represent on average the 8.8% ± 0.1% of all sequences in Oligo1 cycle 9 and the 8.5% ± 0.1% in its replica, thus indicating a statistical compatibility within 3 standard deviations (calculated on the 20 subsamples). Notably, across the 20 subsampling, for each of the analyzed condition, the 10 most abundant sequences are almost always the same. In particular, the first 8/9 are always the same, possibly shuffled. This result should be compared with the top-10 fraction in cycle 10, which is 13.6% ± 0.1%, far beyond the statistical compatibility with cycle 9, with cycle 9 replica and with the distance between the two.

Appendix 2 Further analyses of the Eco-Evolutionary Model

We here show some further results and sensitivity analyses of the Eco-Evolutionary stochastic individual based model. In Figure 2-figure supplement 7 we show how the eco-evolutionary model can describe the emergent order and complexity, that is a loss of the initial huge diversity of the random strings towards few dominating species, during evolution. This behaviour can be quantified 1) by the ratio CR between the zipped file size ***Benedetto et al. (2002***) and the original file size of all the sequences oligomers in the ecosystem or 2) by computing the Shannon entropy of the Relative Species Abundance ***Hill (1973***). We can see that that the model is able to reproduce, at least qualitatively, the marked decrease of diversity observed during evolution.

In Figure 2-figure supplement 8a we show the outcome of the model if we do not include the saturation at ω_{th} = 10. As we can see, the effect is evident as after a few cycles the experimental $\langle\omega\rangle$ *lies sig*nificantly under the model (which promotes too much the strongest sequences). Simi-larly, Figure 2-figure supplement 8b shows the evolution for the average MCO in the case we use only γ = 1 in the simulation (here, ω_{sat} = 11). It is very apparent how in this case the simulated initial evolution is much slower with respect to the observed from the data, while the final trend is

captured. These results indicate that both saturation and the non-linear fitness time dependent fitness function are fundamental ingredients to describe the empirical evolution of $\langle\omega\rangle$. Note that in both cases of the above picture, there is a 10% random sampling drift.

Finally, Figure 2-figure supplement 9a and Figure 2-figure supplement 9b show the simulations results for different total number of individuals ($N = 10^6$, 10^5 and 10^4) and resources ($R = N100$, keeping this ratio fixed) and for different initial conditions (i.e., different sequences populations), respectively. We can see that the qualitative results concerning $\langle\omega\rangle$as a function of time are robust, beyond a given system's size (the silver data in Figure 2-figure supplement 9a are already of a system's size large enough, while the blue ones correspond to a too small system). Considering a different initial (random) population of sequences, keeping fixed all the other hyperparameters (in particular $N = 10^6$ and $R = 1064$), as shown by Figure 2-figure supplement 9b preserves the qualitative agreement with the experimental data, assessing the substantial independence on the initial conditions. Overall, these further analyses show the robustness of the qualitative behavior of results of the Eco-Evolutionary model, pointing out to two relevant phases of the evolution of the oligomers, as highlighted in the main text.

Further results on the interactions between oligomers

In this section we highlight some further results on the interactions between species and resources and among oligemers, respectively.

Figure 4-figure supplement 1 shows the average pair-wise interactions between 10 random strings (as representative of the whole population) during the different evolutionary cycles ($t = 0, 9, 18, 24$), $\langle\Delta G_{pp}\rangle$. Such averages have been computed by giving to NUPACK a pool of 1000 sequences, randomly subdivided in 100 groups of 10 sequences each. We can see that, during evolution, the selected oligomers increase their average interaction strength, a signature that the evolution favors not only strings that have higher overlap with the resource, but also that interact in some way with the other species.

Figure 4-figure supplement 2 is the 2D probability distribution $p(\omega, x_R)$, computed from experimental data, to simultaneously have a given MCO= ω and x_R, the rightmost basis of the of the resource involved in the formation of such an MCO. Noticeably, we start from a distribution peaked in $\omega = 4$ and $10 \leq x_R \leq 12$, essentially corresponding to purely random binding. Across cycles, the probability distribution is deeply modified, with a shift towards the bottom right corner. Along the horizontal axis this simply reflects the shift in the average $\langle\omega\rangle$ *of the p*opulation, and also the fact that winners have large overlaps. Interestingly, we observe significant shift of x_R towards high values, meaning the MCO are preferably formed far away from the bead surface, near the free end of target strands.

Results of the experimental replica

In Figure 2-figure supplement 5 and Figure 2-figure supplement 6 show the main outcomes of the replica experiment Oligo2. The evolution of the average MCO$\langle\omega\rangle$ *over cy*cles is qualitatively the same of that one found in Oligo1: we have a initial steep grow $\langle\omega\rangle$, *compat*ible with a non linear fitness, and then we observe a slower increase for the last cycles, saturating for $\langle\omega\rangle \approx 7$. The histogram shows the whole $p(\omega)$ at cycles $t = 0$ and $t = 18$. As for what we found in O *o1, at* $t = 0$ the behaviour of $p(\omega)$ is compatible with our null random model, while at $t = 18$ the oligomers with higher ω are selected, and the tail of $p(\omega)$ is fatter than the one expected by chance.

These results show that indeed the main outcome of Oligo1 are replicated by Oligo2.

Appendix 3 A combinatorial null model with no evolution

As a first step to understand what happens in our experiments, we have built a null model, assuming purely random attachment sites, i.e. there is not any search for the relative positions of binding filaments so to maximize the MCO. In this way we have a null expectation for the typical MCO distribution in case of oligomers insensitive to the presence of target sequences.

Let us call a the number of consecutive bonded pairs between oligomers 1 (e.g. the species) and 2 (e.g. the resource), with $\max_r 1,2\ MCO = \omega$ and $R_{1,2}$ being the relative position of the left ends of the two filaments, as also explained in ***Mambretti et al. (2022b)*** and in the main text. Consider the initial population being uniformly random selected (in the high 4^L dimensional space of all possible DNA strands). The first quantity we are interested to calculate is $\pi(a)$, the *probability density of a* at time $t = 0$, i.e. before the evolution starts. This distribution is also the distribution of the subsample (i.e, the $\approx 10^6$ strands which we are able to sequence at each cycle), if we assume purely random attachment (no competition among the DNAi, no optimization of the attachment site).

The relative position of the two strands is important since the target can be either “inside” (Figure 3-figure supplement 1, panel a)) or surpassing one of the borders (Figure 3-figure supplement 1, panel b) and C)) of the longer oligomer after the attachment. In the picture, $R_{1,2} = 0$ when the first nucleotide of the target resource overlaps with the first one of the DNAi species. From now on, we will refer to $R_{1,2}$ simply as R.

Our goal consists in finding the MCO of L-long strand (the species) with a l-long target ssDNA (the resource), where $l < L$. In the following calculations, we therefore assume that R is a random uniform variable ($-l + 1 \leq r \leq L - 1$) and we will calculate a_R (for this R).

Such a problem is sketched in Figure 3-figure supplement 2 (where $R = 2$, but the following holds for any R in the allowed range), where we indicate with d the number of mismatching bases between the target resource (red) and the DNAi species (blue), with u the number of matching ones, being $d+u := l$. Labeling as x_i the number of consecutive matching nucleotides comprised between two consecutive mismatching bases, as shown in the picture, the problem can be reformulated in terms of counting how many integer solutions can be found for the equation:

$$\sum_{i=0}^{d} x_i = u \qquad (1)$$

that corresponds to determine the number of ways in which a set of x_i solving Eq. 1 can be obtained. Note that x_i vanishes between two neighboring pairs of mismatching sites, as marked by the arrows in the picture. In the case reported in the picture, e.g., $x_i = (1, 0, 1, 4, 0, 4, 0, 0, 2)$ and $\sum_{i=0}^{8} x_i = 12$, $u = 12$ and $d = 8$.

Ref. ***Charalambides (2008)*** provides us with a formula to answer this question. We stress that finding the number of solutions $A_{d,u}$ for the above equation is equivalent to obtaining the probability distribution $\pi(a)$ for the relative occurrence of each a in a sample of DNA strands, with uniformly random extracted relative positions of the two sequences.

Theorem 1.

Let us have the equation $\sum_{i=1}^{n} x_i = u$ *. Let us suppose that* $s_i \le x_i \le m_i$, $\forall i = 1, \ldots, n$ *for given integers* s_i, m_i, $i = 1, \ldots, n$ *with* $s \le u \le m$, *being* $s := \sum_{i=1}^{n} s_i$, *and* $m = \sum_{i=1}^{n} m_i$ *. Let us define* $w_i = m_i - s_i \ge 0$ $\forall i$. *The number of integer solutions, having the shape* $(r_1, \ldots, r_n)$, *of this equation, with the restrictions aforementioned, is given by:*

$$A_{n,u}(w_1, \ldots, w_n) = \binom{n+u-s-1}{n-1} + \sum_{r=1}^{n} (-1)^r \sum_{\{i_1, i_2, \ldots, i_r\}} \binom{n+u-s-\left(\sum_{j=i_1}^{i_r} w_j\right)-r-1}{n-1} \tag{2}$$

where the inner sum is performed over all the r−combinations (having the shape $\{i_1, i_2, \ldots, i_r\}$) of the n indices $1, \ldots, n$.

In our case, the resource string may not go beyond the DNAi species boundaries (as the latter is longer than the former). But we can modify the name of some variables to adapt the theorem to our problem and make some constraints explicit:

- From $i = 1, \ldots, n$ it follows that $n = d + 1$ because we have $d + 1$ terms (from 0 to d).
- $s_i = 0$ $\forall i$, because each $x_i \ge 0$ by definition. Therefore, $s = 0$.
- At least one of the x_i must be equal to a.
- In principle, m_i is equal to a for each i (which means that there are no consecutive overlaps larger than a).
- It must be that $a \le u \le \min((d+1)a, l)$ (i.e., the total overlap u - which, at most, is equal to $d + 1$ times a - must not be larger than l).

In fact, by using $s = 0$ and $d + u = l$, the theorem Eq. 2 can be rewritten as:

$$A_{d+1,u}(w_1, \ldots, w_n) = \binom{l}{d} + \sum_{r=1}^{d+1} (-1)^r \sum_{\{i_1, i_2, \ldots, i_r\}} \binom{l-\left(\sum_{j=i_0}^{i_r} w_j\right)-r}{d}$$

where the inner sum can be replaced by $\binom{d+1}{r}$ (how many ways are there to dispose the d +1 integer indexes to form r groups):

$$A_{d+1,u}(w_1, \ldots, w_n) = \binom{l}{d} + \sum_{r=1}^{d+1} (-1)^r \binom{d+1}{r} \binom{l-\left(\sum_{j=i_0}^{i_r} w_j\right)-r}{d}$$

First of all, $\binom{l}{d}$ can be placed inside the summation because it corresponds to the r case. Now, we have to apply the constraint that at least one of the $w_j = a$, which means having the first term where the w_j are always equal to a, minus the second term which includes all the cases where all the $w_j < a$:

$$A_{d+1,u}(w_1,\dots,w_n) = \sum_{r=0}^{d+1}(-1)^r\binom{d+1}{r}\binom{l-ra-r}{d} - \sum_{r=0}^{d+1}(-1)^r\binom{d+1}{r}\binom{l-r(a-1)-r}{d} = \sum_{r=0}^{d+1}(-1)^r\binom{d+1}{r}\binom{l-r(a+1)}{d} - \sum_{r=0}^{d+1}(-1)^r\binom{d+1}{r}\binom{l-ra}{d}$$

Note that the previous expressions concern only the cases where $0 \le R \le L - l$. However, this should not matter for practical purposes because R does not appear in the above expressions. Similar formulas can be found when the target surpasses the left/right border: if $-l + 1 \le R \le -1$

$$A_{d+1,u}(w_1,\dots,w_n)^{(II)} = \sum_{r=0}^{d+1}(-1)^r\binom{d+1}{r}\binom{l+R-r(a+1)}{d} - \sum_{r=0}^{d+1}(-1)^r\binom{d+1}{r}\binom{l+R-ra}{d}$$

while if $L - l \le R \le L - 1$

$$A_{d+1,u}(w_1,\dots,w_n)^{(III)} = \sum_{r=0}^{d+1}(-1)^r\binom{d+1}{r}\binom{L-R-r(a+1)}{d} - \sum_{r=0}^{d+1}(-1)^r\binom{d+1}{r}\binom{L-R-ra}{d}$$

Using all the previous results, the general equation for the number of ways which lead to a MCO a is given by:

$$n(a,R) = \sum_{k=1}^{3} n_k(a,R) \tag{3}$$

where the 3 options are originated by the 3 options for the relative position of the target and of the DNAi sketched in Figure 3-figure supplement 1.

Let us now derive n_k, $\forall k$. In particular, if the target resource is completely within the DNAi species boundaries, then we have

$$n_1(a,R) = n_1(a) = (L-l+1)4^{L-l}\sum_{d=0}^{l} 3^d n_{1,d}(a), \tag{4}$$

with $(L-l+1)$ is the total number of possible positions R where the DNAi can attach to the resource, 4^L is the number of ways to build a L-long string (i.e. all possible species), 3^d represents the number of arrangements for the non-matching bases (3 is because we exclude the only matching base) and $n_{1,d}(a) = A^{(I)}_{d+1,u}$ for $0 \le R \le L - l$.

Analogously,

$$n_2(a, R) = \sum_{R=-l+1}^{-1} 4^{L-l-R} \sum_{d=0}^{l+R} 3^d n_{2,d}(a, R), \tag{5}$$

where the summations run over the admitted integer R values as well as over the allowed d values. In this case, 4^{L-l-R} is the number of ways in which the nucleotides not involved in the attachment can be obtained. Here, $n_{2,d}(a, R) = A^{(II)}_{d+1,u}$. A similar equation holds for n_3 *(a)*, where

$$\sum_{R=L-l+1}^{L-1} 4^R \sum_{d=0}^{L-R} 3^d n_{3,d}(a, R)$$

and $n_{3,d}(a, R) = A^{(III)}_{d+1,u}$.

To get the distribution of the overlap measure $\pi(a)$, it suffices to divide $n(a, R)$ by the total number of ways in which we can build a string, i.e. 4^L times the number of possible positions R where the attachment can happen, i.e. $L + l - 1$.

$$\pi(a) := \frac{n(a, R)}{\sum_{j=0}^{l} n(j, R)} = \frac{n(a, R)}{4^L (L + l - 1)} \tag{6}$$

π(a) is exactly the probability density to find a given MCO= a between a l-long and a L-long sequence which found themselves attached in a random position R.

The underlying probability distribution $\pi(a)$ is naturally discretized and can be represented as an histogram, with the occupancy probability for each bin a (the affinity to the resource). $\pi(a)$ is represented in Figure 3-figure supplement 3a as orange bars; grey bars in the same panel represent the average of 50 independent simulations with $K = 10^6$ 50-mers uniformly generated, where their overlap with the target strand - once uniformly random extracted their relative position - is measured.

The analytical result for the null model and simulations yield almost exactly the same results, with the difference that for large MCO we have strong sampling effect in the simulations. In order to understand how possible biases in the initial frequency of each nucleotide in the starting population, we run $N = 50$ independent simulations with a non-uniform frequency for A,C,G,T in the sequences. For instance, the panel **b)** of Figure 3-figure supplement 3 compares the $\pi(a)$ obtained with A,C,G,T having a probability of 25% (grey data) with the corresponding distribution obtained having: A=23%, C=19%, G=29%, T=29%. The average bin occupancy does not change significantly, but only the large a tails are slightly affected by the bias and the error-bars are much larger for the majority of the a values.

We furthermore set a threshold T to model the physical constraint that if $a < T$, the two ssDNAs cannot bind. We thus obtain a **null model physically constrained** distribution $\pi'(a)$, where $\pi'(a) = 0$ if $a < T$, while is the same as before (after a proper normalization) for $a \geq T$. The new analytical distribution $\pi'(a)$ reads as

$$\pi'(a) = \frac{\pi(a) \times \frac{1}{2}[\mathrm{sgn}(a - T) + 1]}{\sum_{j=T}^{l} \pi(j)}, \tag{7}$$

where sgn(0) := 0. The corresponding pseudo-algorithm to generate random number from such distribution is

- sample a random number z from $\pi(a)$
- if $z < T$, sample another number from $\pi(a)$
- else, save it in the new distribution $\pi'(a)$

The comparison between analytical and numerical results are reported in Figure 3-figure supplement 4a and Figure 3-figure supplement 4b (linear and logarithmic scale on y axis, respectively). The cyan bars correspond to the analytical distribution for the null model with physical constraint ($\pi'(a)$), whereas the purple bars represented the average over $N = 200$ independent simulations of $\pi'(a)$ performed via Metropolis Monte Carlo accept-reject technique ***Metropolis et al. (1953***). A custom Python script which simulates this process is available at the GitHub repository associated to this work. The null model that we present in the main text is the physical constraint one, i.e. $\pi'(a)$.

References

Adamala K, Szostak JW (2013) **Competition between model protocells driven by an encapsulated catalyst** *Nature Chemistry* **5**:495–501 https://doi.org/10.1038/nchem.1650

de Aguiar MAM, Baranger M, Baptestini EM, Kaufman LS, Bar-Yam Y. (2009) **Global patterns of speciation and diversity** *Nature* **460**:384–387

Anceschi N, Hidalgo J, Bellini T, Maritan A, Suweis S. (2018) **How neutral and niche forces contribute to speciation processes** *arXiv: Populations and Evolution*

Andreetto P *et al.* (2019) **Merging OpenStack-based private clouds: the case of CloudVeneto.it** *EPJ Web of Conferences*

Benedetto D, Caglioti E, Loreto V. (2002) **Language trees and zipping** *Physical Review Letters* **88**

Bohlin J, Matthies M, Poppleton E, Procyk J, Mallya A, Yan H, Šulc P. (2022) **Design and simulation of DNA, RNA and hybrid protein–nucleic acid nanostructures with oxView** *Nature Protocols* **17**:1762–1788 https://doi.org/10.1038/s41596-022-00688-5

Camacho Mateu J, Sireci M, Muñoz MA (2021) **Phenotypic-dependent variability and the emergence of tolerance in bacterial populations** *PLoS computational biology* **17**

Catalán P, Arias CF, Cuesta JA, Manrubia S. (2017) **Adaptive multiscapes: an up-to-date metaphor to visualize molecular adaptation** *Biology Direct* **12**:1–15

Charalambides CA (2008) **Enumerative Combinatorics** *SIGACT News* **39**:25–27 https://doi.org/10.1145/1466390.1466395

Chase JM, Leibold MA (2009) **Ecological niches**

Mayr Davis WB. (1943) **Ernst. Systematics and the Origin of Species** :273–274 https://doi.org/10.2307/1374810

De Visser JAG, Krug J. (2014) **Empirical fitness landscapes and the predictability of evolution** *Nature Reviews Genetics* **15**:480–490

Di Leo S, Marni S, Plata CA, Fraccia TP, Smith GP, Maritan A, Suweis S, Bellini T. (2022) **Pairing statistics and melting of random DNA oligomers: Finding your partner in superdiverse environments** *PLoS computational biology* **18**

Dieckmann U, Doebeli M. (1999) **On the origin of species by sympatric speciation** *Nature* **400**:354–357

Dirks RM, Bois JS, Schaeffer JM, Winfree E, Pierce NA (2007) **Thermodynamic Analysis of Interacting Nucleic Acid Strands** :65–88 https://doi.org/10.1137/060651100

Ellington AD, Szostak JW (1990) **In vitro selection of RNA molecules that bind specific ligands** *Nature* **346**:818–822 https://doi.org/10.1038/346818a0

Fornace ME, Porubsky NJ, Pierce NA (2020) **A Unified Dynamic Programming Framework for the Analysis of Interact-ing Nucleic Acid Strands: Enhanced Models, Scalability, and Speed** *ACS Synthetic Biology* **9**:2665–2678 https://doi.org/10.1021/acssynbio.9b00523

Fussmann GF, Loreau M, Abrams PA (2007) **Eco-evolutionary dynamics of communities and ecosystems** *Functional ecology* :465–477

Ghosh S, Takahashi S, Endoh T, Tateishi-Karimata H, Hazra S, Sugimoto N. (2019) **Validation of the nearest-neighbor model for Watson–Crick self-complementary DNA duplexes in molecular crowding condition** *Nucleic acids research* **47**:3284–3294

Gupta D, Garlaschi S, Suweis S, Azaele S, Maritan A. (2021) **Effective resource competition model for species coexistence** *Physical review letters* **127**

Hill MO (1973) **Diversity and evenness: a unifying notation and its consequences** *Ecology* **54**:427–432

Ichihashi N, Usui K, Kazuta Y, Sunami T, Matsuura T, Yomo T. (2013) **Darwinian evolution in a translation-coupled RNA replication system within a cell-like compartment** *Nature Communications* **4** https://doi.org/10.1038/ncomms3494

Katla SK, Lin C, Pérez-Mercader J. (2023) **Competitive exclusion principle among synthetic non-biochemical protocells** *Cell Reports Physical Science* **4** https://doi.org/10.1016/j.xcrp.2023.101359

Kauffman WB, Guha S, Wimley WC (2018) **Synthetic molecular evolution of hybrid cell penetrating peptides** *Nature Communications* **9** https://doi.org/10.1038/s41467-018-04874-6

Keymer JE, Fuentes MA, Marquet PA (2012) **Diversity emerging: from competitive exclusion to neutral coexistence in ecosystems** *Theoretical Ecology* **5**:457–463

Levin SA (1970) **Community equilibria and stability, and an extension of the competitive exclusion principle** *The American Naturalist* **104**:413–423

Mambretti F, Pedrani N, Casiraghi L, Paraboschi EM, Bellini T, Suweis S. (2022) **OxDNA to Study Species Interactions** *Entropy* **24** https://doi.org/10.3390/e24040458

Mambretti F, Pedrani N, Casiraghi L, Paraboschi EM, Bellini T, Suweis S. (2022) **OxDNA to Study Species Interactions** *Entropy* **24** https://doi.org/10.3390/e24040458

Message Passing Interface Forum (2021) **Message Passing Interface Forum. MPI: A Message-Passing Interface Standard Version 4.0; 2021, https://www.mpi-forum.org/docs/mpi-4.0/mpi40-report.pdf.**

Metropolis N, Rosenbluth AW, Rosenbluth MN, Teller AH, Teller E. (1953) **Equation of state calculations by fast computing machines** *J Chem Phys* **6** https://doi.org/10.2172/4390578

Parrilla-Gutierrez JM, Tsuda S, Grizou J, Taylor J, Henson A, Cronin L. (2017) **Adaptive artificial evolution of droplet protocells in a 3D-printed fluidic chemorobotic platform with configurable environments** *Nature Communications* **8** https://doi.org/10.1038/s41467-017-01161-8

Peterson AT (2011) **Ecological niche conservatism: A time-structured review of evidence** *Journal of Biogeography* **38**:817–827

Pigolotti S, López C, Hernández-García E. (2007) **Species clustering in competitive Lotka-Volterra models** *Phys Rev Lett* https://doi.org/10.1103/PhysRevLett.98.258101

Plata CA, Marni S, Maritan A, Bellini T, Suweis S. (2021) **Statistical physics of DNA hybridization** *Physical Review E* **103**

Poppleton E, Bohlin J, Matthies M, Sharma S, Zhang F, Šulc P. (2020) **Design, optimization and analysis of large DNA and RNA nanostructures through interactive visualization, editing and molecular simulation** *Nucleic Acids Res* **48**

Rundle H, Nosil P. (2005) **Ecological speciation - Rundle - 2005 - Ecology Letters - Wiley Online Library** *Ecology letters* **1**

Sanderson C, Curtin R. (2016) **Armadillo: a template-based C++ library for linear algebra** *Journal of Open Source Software* **1** https://doi.org/10.21105/joss.00026

Sanderson C, Curtin R., Davenport JH, Kauers M, Labahn G, Urban J (2018) **A User-Friendly Hybrid Sparse Matrix Class in C++** *Mathematical Software – ICMS 2018* :422–430

SantaLucia J. (1998) **A unified view of polymer, dumbbell, and oligonucleotide DNA nearest-neighbor thermody-namics** *Proceedings of the National Academy of Sciences* **95**:1460–1465

Solé R (2016) **The major synthetic evolutionary transitions** *The Royal Society*

Thurner S, Hanel R, Klimek P. (2010) **Physics of evolution: Selection without fitness** *Physica A: Statistical Mechanics and its Applications* **389**:747–753

Tizei PAG, Csibra E, Torres L, Pinheiro VB (2016) **Selection platforms for directed evolution in synthetic biology** *Biochemical Society Transactions* **44**:1165–1175 https://doi.org/10.1042/bst20160076

Tolle F, Wilke J, Wengel J, Mayer G. (2014) **By-product formation in repetitive PCR amplification of DNA libraries during SELEX** *PloS one* **9**

Tuerk C, Gold L. (1990) **Systematic Evolution of Ligands by Exponential Enrichment: RNA Ligands to Bacteriophage T4 DNA Polymerase** *Science* **249**:505–510 https://doi.org/10.1126/science.2200121

Vetsigian K. (2017) **Diverse modes of eco-evolutionary dynamics in communities of antibiotic-producing microorgan- isms** *Nature Ecology & Evolution* **1**

Wiser MJ, Lenski RE (2015) **A comparison of methods to measure fitness in Escherichia coli** *PloS one* **10**

Woodside MT, Behnke-Parks WM, Larizadeh K, Travers K, Herschlag D, Block SM (2006) **Nanomechanical measurements of the sequence-dependent folding landscapes of single nucleic acid hairpins** *Proceedings of the National Academy of Sciences* **103**:6190–6195

Zadeh JN, Steenberg CD, Bois JS, Wolfe BR, Pierce MB, Khan AR, Dirks RM, Pierce NA (2011) **NUPACK: Analysis and design of nucleic acid systems** *J Comput Chem* **32**:170–173

Article and author information

Luca Casiraghi
Dipartimento di Biotecnologie Mediche e Medicina Traslazionale, Università degli Studi di Milano, Via Fratelli Cervi, 93 - L.I.T.A., Segrate, 20054, Italy

Francesco Mambretti
Dipartimento di Fisica e Astronomia, Università degli Studi di Padova, Via Marzolo 8, Padova, 35131, Italy
ORCID iD: 0000-0002-3712-3595

Anna Tovo
Dipartimento di Fisica e Astronomia, Università degli Studi di Padova, Via Marzolo 8, Padova, 35131, Italy

Elvezia Maria Paraboschi
Department of Biomedical Sciences, Humanitas University, Via Rita Levi Montalcini 4, Pieve Emanuele, 20072, Italy, IRCCS, Humanitas Clinical and Research Center, Via Manzoni 56, Rozzano, 20089, Italy
For correspondence: elvezia_maria.paraboschi@hunimed.eu

Samir Suweis
Dipartimento di Fisica e Astronomia, Università degli Studi di Padova, Via Marzolo 8, Padova, 35131, Italy
For correspondence: samir.suweis@unipd.it
ORCID iD: 0000-0002-1603-8375

Tommaso Bellini
Dipartimento di Biotecnologie Mediche e Medicina Traslazionale, Università degli Studi di Milano, Via Fratelli Cervi, 93 - L.I.T.A., Segrate, 20054, Italy
For correspondence: tommaso.bellini@unimi.it

Copyright

Editors

Reviewing Editor
Anne-Florence Bitbol
Ecole Polytechnique Federale de Lausanne (EPFL), Lausanne, Switzerland

Senior Editor
Aleksandra Walczak
École Normale Supérieure - PSL, Paris, France

Reviewer #1 (Public Review):

This work describes a new and powerful approach to a central question in ecology: what are the relative contributions of resource utilisation vs interactions between individuals in the shaping of an ecosystem? This approach relies on a very original quantitative experimental set-up whose power lies in its simplicity, allowing an exceptional level of control over ecological parameters and of measurement accuracy.

In this experimental system, the shared resource corresponds to 10^12 copies of a fixed single stranded target DNA molecule to which 10^15 random single stranded DNA molecules (the individuals populating the ecosystem) can bind. The binding process is cycled, with a 1000x-PCR amplification step between successive binding steps. The composition of the population is monitored via high-throughput DNA sequencing. Sequence data analysis describes the change of population diversity over cycles. The results are interpreted using estimated binding interactions of individuals with the target resource, as well as estimated binding interactions between individuals and also self-interactions (that can all be directly predicted as they correspond to DNA-DNA interactions). A simple model provides a framework to account for ecosystem dynamics over cycles. Finally, the trajectory of some individuals with high frequency in late cycles is traced back to the earliest cycles at which they are detected by sequencing. Their propensities to bind the resource, to form hairpins or to form homodimers suggest how different interaction modes shape the composition of the population over cycles.

The authors report a shift from selection for binding to the resource to interactions between individuals and self-interactions over the course of cycles as the main driver of their ecosystem. The outcome of the experiment is far from trivial as the individual-resource binding energy initially determines the relative enrichment of individuals, and then seems to saturate. The richness of the population dynamics observed with this simple system is thus comparable to that found in some natural ecosystems. The findings obtained with this new approach will likely guide the exploration of natural ecosystems in which parameters and observables are much less accessible.

My review focuses mainly on experimental aspects of this work given my own expertise. The introduction exposes very convincingly the scientific context of this work, justifying the need for such an approach to address questions pertaining to ecology. The manuscript describes very clearly and rigorously the experimental set-up. The main strengths of this work are (i) the outstanding originality of the experimental approach and (ii) its simplicity. With this setup, central questions in ecology can be addressed in a quantitative manner, including the possibility to run trajectories in parallel to generalize the findings, as reported here. Technical aspects have been carefully implemented, from the design of random individuals bearing flanking regions for PCR amplification, binding selection and (low error) amplification protocols, and sequencing read-out whose depth is sufficient to capture the relevant dynamics. With this setup one can tune the relative contributions of binding selection vs amplification for instance (to disentangle forces that shape the ecosystem). One can also run cycles with new DNA individuals, designed with arbitrarily chosen resource binding vs self-binding, that are predicted to dominate depending on chosen ecological parameters. These exciting perspectives underlie the strong potential of the new approach described in the current study.

https://doi.org/10.7554/eLife.90156.2.sa1

Reviewer #2 (Public Review):

Summary:
In this manuscript, the authors introduced ADSE, a SELEX-based protocol to explore the

mechanism of emergency of species. They used DNA hybridization (to the bait pool, "resources") as the driving force for selection and quantitatively investigated the factors that may contribute to the survival during generation evolve (progress of SELEX cycle), revealing that besides individual-resource binding, the inter- and intra-individual interactions were also important features along with mutualism and parasitism.

Strengths:
The design of using pure biochemical affinity assay to study eco-evolution is interesting, providing an important viewpoint to partly explain the molecular mechanism of evolution.

https://doi.org/10.7554/eLife.90156.2.sa0

Author Response

The following is the authors' response to the original reviews.

> ***Reviewer #1:***
>
> *This work describes a new and powerful approach to a central question in ecology: what are the relative contributions of resource utilisation vs interactions between individuals in the shaping of an ecosystem? This approach relies on a very original quantitative experimental set-up whose power lies in its simplicity, allowing an exceptional level of control over ecological parameters and of measurement accuracy.*
>
> *In this experimental system, the shared resource corresponds to 10^12 copies of a fixed single-stranded target DNA molecule to which 10^15 random single-stranded DNA molecules (the individuals populating the ecosystem) can bind. The binding process is cycled, with a 1000x-PCR amplification step between successive binding steps. The composition of the population is monitored via high-throughput DNA sequencing. Sequence data analysis describes the change in population diversity over cycles. The results are interpreted using estimated binding interactions of individuals with the target resource, as well as estimated binding interactions between individuals and also self-interactions (that can all be directly predicted as they correspond to DNA-DNA interactions). A simple model provides a framework to account for ecosystem dynamics over cycles. Finally, the trajectory of some individuals with high frequency in late cycles is traced back to the earliest cycles at which they are detected by sequencing. Their propensities to bind the resource, to form hairpins, or to form homodimers suggest how different interaction modes shape the composition of the population over cycles.*
>
> *The authors report a shift from selection for binding to the resource to interactions between individuals and self-interactions over the course of cycles as the main drivers of their ecosystem. The outcome of the experiment is far from trivial as the individual resource binding energy initially determines the relative enrichment of individuals, and then seems to saturate. The richness of the population dynamics observed with this simple system is thus comparable to that found in some natural ecosystems. The findings obtained with this new approach will likely guide the exploration of natural ecosystems in which parameters and observables are much less accessible.*
>
> *My review focuses mainly on the experimental aspects of this work given my own expertise. The introduction exposes very convincingly the scientific context of this work, justifying the need for such an approach to address questions pertaining to ecology. The manuscript describes very clearly and rigorously the experimental setup. The main strengths of this work are (i) the outstanding originality of the experimental approach and (ii) its simplicity. With this setup, central questions in ecology can be addressed in a quantitative manner, including the possibility of running trajectories in parallel to*

> *generalize the findings, as reported here. Technical aspects have been carefully implemented, from the design of random individuals bearing flanking regions for PCR amplification, binding selection and (low error) amplification protocols, and sequencing read-out whose depth is sufficient to capture the relevant dynamics.*
> *:*
> *We thank the reviewer for summarizing our work and the main findings in a very clear and effective manner.*
>
> *One missing aspect in the data analysis is the quantification of the effect of PCR amplification steps in shaping the ecosystem (to be modeled if significant). In addition, as it stands the current work does not fully harness the power of the approach. For instance, with this setup, one can tune the relative contributions of binding selection vs amplification for instance (to disentangle forces that shape the ecosystem). One can also run cycles with new DNA individuals, designed with arbitrarily chosen resource binding vs self-binding, that are predicted to dominate depending on chosen ecological parameters. I have three main recommendations to the authors:*
>
> 1. *PCR amplification steps (and not only binding selection steps) should be taken into account when interpreting the outcome of experiments.*
>
> 1. *More generally, a systematic analysis of the possible modes of propagation of a DNA molecule from one cycle to the next, including those considered as experimental noise, would help with interpreting the results.*
>
> 1. *Testing experimentally the predictions from the analysis and the modelling of results would strengthen the case for this approach.*

Despite its conceptual simplicity, our approach has indeed a few experimental handles that enable exploring a relevant variety of conditions much beyond those described in this paper, of which we are very aware. These involve selection vs. amplification or set the stage to explore competition, parasitism or cooperation among specific species, as the reviewer points out, but also introduce mutations and explore the kinetics of evolution in static or dynamic environments. Ongoing experiments are considering some of these conditions. We modified the text to mention more explicitly these possibilities, which are now mentioned in p11 lines 376-378 and lines 416-417. The three points raised by the reviewer helped us to further improve and clarify strengths and limitations of our work, as detailed below.

> *Regarding the first point, here are my suggestions :*
>
> - *Run one cycle of just amplification vs 'binding + amplification', or simply increase the number of PCR cycles (and subsample the product) to check whether it impacts the population composition, in particular for sequences with predictions derived from the current analysis.*

The point raised by the reviewer is indeed very relevant and not discussed in our manuscript. Prompted by the reviewer's comment, we performed two new experiments to distinguish resource-binding selection from PCR amplification effects.

First, we performed a negative control experiment in which we performed the "selection step" with bear beads, i.e. beads without with no DNA grafted on them. We then compared the results with the corresponding results of the original experiments on Oligo 1 and 2.

After 6 cycles, the most abundant sequence in the negative dataset has a relative occurrence of 0.05%, whereas the dominant strand in Oligo 1 and Oligo 2 has an abundance of 8% and 16%, respectively, i.e. 40-80 times larger.

This indicates that the drift due to non-specific binding + PCR amplification is at least two orders of magnitude smaller than the selection induced by the affinity with the resource.

This results are now cited in p14 lines 468-470, and described in Appendix 1, Experimental controls.

Second, we tested the effect of PCR amplification on the selection process. We exploited the fact that we have aliquots for each generation of our evolution experiment, which we sampled and saved after PCR and before sequencing. We thus chose a specific generation - specifically generation 9 from Oligo 1 experiments - and performed another PCR round we proceeded directly to sequencing with no beadsselection step. We then compared the ensemble of oligos obtained in this way, which we named Oligo 1 “cycle 9 replica”, with both the original Oligo1 cycle 9, and with Oligo1 cycle 10.

We sampled 20 times 4 x 10^5 sequences from the cycle 9 dataset, from cycle 9 replica and from cycle 10 with a bootstrap approach. To compare the three systems we extracted the fraction of the population of each covered by the 10 most abundant individuals. The results are shown in Figure 2 - Figure Supplement 4. In the figure caption further details on the analysis can be found. The similarity between cycle 9 and cycle 9 replica and the marked difference between cycle 9 replica and cycle 10

indicates that the relevant part of the selection is indeed performed by the resourcebinding mechanism, while drifts induced by PCR play a secondary role.

As a further check, we compared the specific sequences across the 20 samples in cycle 9 and cycle 9 replica datasets and found that the 10 most abundant sequences are almost always the same. In particular, the first 8/9 are always the same, possibly shuffled.

These new pieces of evidence are now cited in p14 lines 483-484 and described in Appendix 1, Experimental controls.

> - *Sequencing read-out includes the same PCR protocol as the one used for amplification steps, so read-out potentially has an effect on the composition of the ecosystem. Again, varying the number of PCR cycles is a direct way to test this.*

The PCR amplification involved in the read-out might have a minor effect on the sequencing outcome but not on the composition of the ecosystem. In fact, the sample that undergoes sequencing is taken from the pool at each cycle, and not inserted back into it. Thus, it does not participate in the following selection steps. This is specified in the text at p3 line 104

> - *Could self-interactions (hairpins of homodimers) benefit individuals during amplification steps? The role of self-interactions during binding selection steps could also be tested directly over one cycle (again varying the relative weight of the binding vs amplification to disentangle both).*

Our choice of conditions for PCR amplification were thought to minimize effects of this type. PCR amplification is carried out at 68 C, a temperature at which, given the level of self and mutual complementarity in the sequences analyzed in the text, hairpins or homodimers should be melted and thus have no effect. This is specified in the text at p. 14 lines 479-480 However, if an effect is present, it gives a disadvantage (rather than an advantage) to self-interacting individuals. For the amplification step we used Q5® Hot Start HighFidelity DNA

Polymerase, which does not possess strand displacement activity. Therefore, in theory, if during amplification the polymerase encounters a double strand portion, it stops and synthesizes only a truncated product, which will be then lost during the purification step. In other words, sequences with secondary and/or tertiary structures are less likely to be amplified during the polymerization step. As a consequence, a DNAi that is characterized by this kind of structures, will be negatively selected even in the case of optimal binding to the resource, and will be underrepresented in the pool.

> *About the second point:*
>
> - *Regarding the effect of sampling (sequencing read-out), PCR amplification errors: explicitly check the consistency of observations with the expected outcome, in the methods section (right now these aspects are only briefly mentioned in the main text), which would highlight again the level of control and accuracy of the system.*

Hoping to have well interpreted the request, we performed a technical replicate sequencing Oligo 1 cycle 9 again and analyzed the sequences that have at least 100 reads (corresponding to 27.42% of the total reads). We find that among the 800 DNA species that have at least 100 reads, 93.6% are found in both replicates. All the nonoverlapping sequences have very low abundance, close to 100.

Moreover, we compare the population size of each DNA species between the two replicas, after having equalized the database sizes. The results are now cited in p14 lines 509-510, In Appendix 1, Experimental Controls and shown in Figure 2-figure supplement 3, where we plot the ratio of the number of reads in the two replicates for each sequence as a function of the number of reads in one. We found an average of 0.965 with a standard deviation of 0.119. High fluctuations are found in the most rare species, as expected.

We think this evaluation indeed strengthens the solidity of our results.

> - *I have a small concern about target resource accessibility: is there any spacer between the ssDNA and the bead? The methods section does not mention any, and I would expect such a proximity between the target DNA and the bead to yield steric repulsion that impedes interactions with random DNA individuals.*

Yes, there is a 12-carbon spacer between the bead and the resource, which was inserted exactly to make the resource more accessible. This information is now available in Table 1 of Supplementary Information detailing the sequences used in the experiment. However, as now described in the text (p8 lines 284-286), we observe that the interaction with the resource is always shifted to the 3', the terminal furthest from the bead, indicating some residual issue of accessibility to the resource sections closest to the bead.

> - *Regardless of the existence of a spacer, binding of random DNA molecules to beads instead of the target DNA constitutes a potential source of noise (described for now as '1-x' in the IBEE model), which can be probed by swapping targets, selecting without target etc.*

This issue is addressed by the test with bare beads described above, in which we found little effects, corresponding to small $1-x$ value.

> - *Is there any recombination potentially occurring during amplification steps? This could be tested with a set of known molecules amplified over 24 amplification steps in a row (no binding step).*

It is possible for recombination to occur during the amplification steps. In Appendix 2, the section "By-Product Formation from PCR Amplification", discusses PCR byproducts as aberrant forms of amplification, such as recombination events. We adopted several strategies to limit by-product formation, such as: i) use of “blockers” characterized by a phosphate group at 3’ end (thus inhibiting their usage during the amplification and allowing a better control of the reaction conditions over the PCR cycles), ii) a high annealing temperature (to limit the possibility of a spurious primer annealing to the random region), iii) fewer PCR cycles, iv) a high primer concentration, v) a very short elongation step (all these strategies have been implemented to avoid a possible mispriming event between different DNAi, and the formation of concatemers). However, the formation of by-products is a problem inherent to the technique: in fact, it is a known issue for classical SELEX technology (Tolle et al. 2014), mainly due to the random region within the DNAi. Q5® Hot Start High-Fidelity DNA Polymerase (New England Biolabs, Ipswich, MA, USA) has an error rate of <0.44 x 10-6/base.

In classic SELEX technology, the average number of selection cycles is 10. This limitation is partly due to the increase in PCR by-products. As we can see from Figure 2 Supplementary Figure 1, the percentage of PCR by-products is less than 20% at cycle 12, and then increases dramatically in the following cycles. We are performing a series of experiments with known and limited sequences to verify and better understand the phenomenon for future applications of the SEDES platform. On this issue we decided not to modify the manuscript since we think it is already well discussed in Appendix 1.

> *And the third point:*
>
> - *Perform one cycle (or a few cycles) with random DNA individuals, the most frequent individuals at the end of the current experiment, newly designed individuals with higher binding affinity to the target than currently dominating individuals, newly designed individuals with higher propensity to form hairpins or to form homodimers. Such experimental testing of predictions from the data analysis/modeling, typical of a physics approach, would illustrate the level of understanding one can reach with a simple yet powerful experimental setup.*

We perfectly agree that the approach we propose and the set of results we obtained call for further investigations that could strengthen analysis and modeling. The final aim we envisage is the understanding, within this simplified approach, of key evolutionary factors such as fitness. Indeed, becoming able to write an explicit fitness function would be a significant new contribution to the understanding of evolutionary processes, even within the limited settings of the ADSE approach, as discussed in the conclusions of the manuscript.

However, undergoing such an analysis is a long and expensive job, which we have started and will be completed in a not immediate future. For this reason, given the already significant body of results we are presenting here, we prefer to keep this paper confined to the study of the evolution of a random DNAi population and discuss in a future contribution the behavior of smaller designed sets of competing, collaborating or parasitic individuals.

Looking ahead, additional stages of investigations will also include mutations - to investigate the kinetics of speciation, and, in an even further stage, the interplay between evolution kinetics and dynamical mutation of resources.

> *I have a few smaller points:*
>
> - *It would be very useful to provide the expected dynamic range of binding free energies (in terms of DeltaG and omega): what is the maximum binding free energy for the perfect complement?*

The NUPACK-computed binding free energy of a 20 basis-long oligomer complementary to the resource (ω=20) is -24.36 Kcal/mol for Oligo1 and -23.08 Kcal/mol for oligo 2. This is the best answer we can offer to the reviewer's request, since the maximum binding free energy of DNAi individuals (much longer than the target strand) would include contributions from the unpaired bases. Indeed, the values give above are approached by the left tail of the distribution of Fig. 3a, which however includes DNAi self-energies.
The perfect complement binding free energy is now cited in the text as a reference for the dynamical range of DeltaG (p4 lines 151-152).

- *How is the number of captured DNA molecules quantified? Is 10^12 measured, estimated, or hypothesized?*

The number of sequences was calculated from data obtained from 260 nm absorbance quantification. We have now added this information in the Methods, Selection Phase" section.

Reviewer #2:

Summary:

In this manuscript, the authors introduced ADSE, a SELEX-based protocol to explore the mechanism of emergency of species. They used DNA hybridization (to the bait pool, "resources") as the driving force for selection and quantitatively investigated the factors that may contribute to the survival during generation evolution (progress of SELEX cycle), revealing that besides individual-resource binding, the inter- and intra-individual interactions were also important features along with mutualism and parasitism.

Strengths:

The design of using pure biochemical affinity assay to study eco-evolution is interesting, providing an important viewpoint to partly explain the molecular mechanism of evolution.

Weaknesses:

Though the evidence of the study is somewhat convincing, some aspects still need to be improved, mostly technical issues.

Major:

1. *There are a few technical issues that the authors should clarify in the manuscript to make the analysis more transparent:*

   1.1) To my understanding, it is difficult to guarantee the even distribution of different species (individuals) in the initial individual pool. Even though the authors have shown in Fig. 2a that the top 10 sequences take up ~ 0% in the pool, it remains unclear how abundant these top and bottom representative sequences are, given the huge number of the pool (10E15). Can the author show the absolute number of these sequences in different quantiles? Please show both Oligo sets.
   : First, we thank the reviewer for both positive and critical comments that have guided us in reformulating or clarifying some messages of our work.

As for this specific point: 10E15 is a small number compared to 4^50 = 10E30, the number of possible sequences of length 30. Thus, we don't expect more than one individual per sequence in the initial pool. However, sequencing requires a preparation amplification, which may lead to detecting a few sequences with more than one individual.

Specifically, in the initial pool of Oligo 1, the most abundant individual (of sequence GAACTAAAGGGGCGGTGTCCACTTGCCTGTAGTGGTTATCAGTCCGGTTG)has 3 copies. The 0.7% of the sequences has 2 copies, while the vast majority of strings (99.3% on a sample of about 1.5 x 10E6 sequenced DNAi) is present in one copy only. A similar situation holds for Oligo 2, with 4 DNAi present in 3 copies and the 0.8% of the sequences (in a pool of 2 x 10E6 DNAi) in 2 copies.

It is worth noticing that none of the 10 most abundant species in the last cycle is present in the sample. Indeed, the fraction of the pool which is sequenced is removed from the population that undergoes evolution (as now specified in p2, line 104). We specified in the text (p2, lines 69-70, p3 lines 94-96) the fact that in the initial pool no sequence is expected to be present in more than one individual.

> *1.2) The author claimed that they used two different oligo sets (Oligo1 and Oligo2) in this study. It is unclear which data was used in the presentation. How reproducible are they? Similar to this concern, how reproducible if the same oligo set was used to repeat the experiment?*

The oligo used in the main text was declared in Methods, Replica section. It is now declared also in the main text (p3 lines 106-108 and in the captions of Figure 2, Figure 3 and Figure 4). Reproducibility is addressed in: Figure 2-figure supplement 5; Figure 2-figure supplement 6; Appendix 2: Results of the experimental replica.

It should also be noted that two starting pools of random 50mers are necessarily disjoint sets for the same reason discussed in the previous answer: the probability of common sequences in two 10E15 selections from a 10E30 is negligibly small. Thus, it is expected that each time a new evolution experiment is started, different dominant sequences are found. However, the statistical properties of the DNAi pool during the evolution process of Oligo1 and Oligo2 are similar as discussed in Appendix 2 of the paper.

> *1.3) PCR and illumina sequencing itself introduced selection bias. How would the analysis eliminate them? The authors only discussed the errors created during PCR cycles (page 3, lines 115-122). However the PCR itself would prefer to amplify some sequences over the others (e.g. with high GC content). Similarly, the illumina sequencing would be difficult to sequence the low complexity sequences. How would this be circumvented?*

Yes, both PCR and Illumina sequencing have some known biases in the amplification process (e.g. sequencing of homopolymers or amplification of GC-rich sequences) that are intrinsic to the used techniques. Regarding PCR, we implemented a thermal protocol optimized for our chosen experimental setup, characterized by very short denaturation, annealing and amplification steps performed at high temperatures. Regarding Illumina sequencing, we can't rule out a bias against specific sequences (e.g, homopolymers), which however should not be captured during the selection step, due to the design of the resource. Also, the libraries subjected to sequencing are characterized by a low complexity: according to the experimental design, the first and last 25 nucleotides are the same for all DNAi, the only differences being in the central 50 nt-long sequence. It is known that a low complexity library might encounter problems during sequencing due to the design of Illumina instruments: nucleotide diversity, especially in the first sequencing cycles, is critical for cluster filtering, optimal run performance and high-quality data generation. To overcome this limitation, the obtained libraries were run together with more complex and diverse library preparations: the ADSE sequences were about 1-2% of the total reads per run, corresponding to only a few million reads.

This discussion is now in Appendix 1, Intrinsic limitations of the molecular approach.

> *1.4) Some DNA sequences would bind to the beads instead of the resource sequence coated on them. Should the author run the experiment using bead alone as a control?*
> *: We performed a negative control experiment in which we performed the "selection step" with bear beads, i.e. beads without with no DNA grafted on them. We then compared the results with the corresponding results of the original experiments on Oligo 1 and 2.*

After 6 cycles, the most abundant sequence in the negative dataset has a relative occurrence of 0.05%, whereas the dominant strand in Oligo 1 and Oligo 2 has an abundance of 8% and 16%, respectively, i.e. 40-80 times larger.

This indicates that the drift due to non-specific binding (+ PCR amplification) is at least two orders of magnitude smaller than the selection induced by the affinity with the resource. This part is now discussed in Appendix 1, Experimental controls.

> *1. It would be interesting to study the impact of environmental factors, for example, changing pH, salt concentration, and detergent. Would these factors accelerate/decelerate the evolution?*

We agree that the approach we propose and the set of results we obtained call for further investigations. However, performing these additional experiments, which would require a minimum of 6 generations each, is a long and expensive job, which we have started and will not be completed in the near future. For this reason, given the already significant body of results we are presenting here, we prefer to keep this paper confined to the study of the evolution of a random DNAi population in the selected conditions and leave the exploration of new conditions, potentially opening new evolutionary scenarios, to a future contribution. In fact, our aim was to show that through our platform we can indeed observe fundamental elements of evolution in a non-biological system, which, in the set of chosen parameters, we do.

> *1. The concentration of individual oligo is apparently one of the most important factors in determining the interactions. In later cycles, some oligos become dominant, namely with extremely higher concentrations compared to their concentration in earlier cycles. This would definitely affect its interaction with resources, or self-interaction, or interaction with other oligos in the pool. However, the authors failed to discuss this factor, which may explain the exponential enrichment in later cycles.*

We agree with the reviewer that this is an important point, but we disagree that we have not discussed it. We introduce the topic at the end of the "Null Model and Eco-evolutionary Algorithm", where we comment on the change of the gamma parameter by saying that there must be a shift in the evolution process, first dominated by the interactions with the resources, and in later stages by some other factors (lines 227230) that we then discuss in "Self and mutual DNAi interactions are evolutionary drivers". In this latter chapter and in the following, we indeed discussed the effects of mutual and self interactions between DNAi.

Indeed, a key point in our paper is the change in the gamma parameter necessary to match the IBEE model to experiments, as it is now more openly stated (p5 lines 217218 where we also mention figure 2-supplement 8 which clearly shows the necessity of a variable gamma). The two regimes enlightened by the gamma value must reflect a change in the competition for the resources and interactions among species. In the first generations, where the diversity of species is large (there are few strings for each species) and binding to the resources generally very week (small), the affinity with the resource is the main driving force (fast growth of), while mutual interactions remain too random to favor any species in particular. In the later cycles instead, when becomes large enough to provide a significant stability to the

resource-binding of the majority of species, the dominating species compete more intensively on the basis of their structure and capacity of self-defense, parasitism and mutualism, a condition in which evolution affects more modifications in sequences than in .

Certainly, our understanding of this shift is based on statistical behavior and it is inferential, based on the study of specific DNAi described in the last part of the manuscript. For a better molecular model, more experiments with selected DNAi competing, cooperating or being parasitic would be necessary, with the final aim of defining a predictive fitness function. Alas, this requires months of further investigation. :

> *1. The author observed the different behaviors of medium ω in early and late cycles, referring to Fig 2h. Using the IBEE model, they found out it is the change of gamma. However, the authors did not further discuss the molecular mechanism. It could be very interesting to understand the evolutionary change of these individuals.*

This comment might be related to the previous one. It is true that our discussion and understanding of the whole process is statistical, and misses a molecular model to predict the value of gamma.

However, the specific behavior that the reviewer asks about (those in Fig. 2h) is not related to the change in gamma. Even if gamma remains as in the first part of the evolution (gamma = 3), the species with overlap between 6 and 10 would first grow in number and later decrease. Indeed, during the first cycles they have an advantage with respect to the majority of species with lower maximum overlap, a condition that favors their amplification. However, in the second stage of the evolution dominant species with a larger affinity emerge and outcompete the individuals of this class. We added a sentence in the text to clarify this point (p7 lines 227-229).

> *1. In Figure 2f, some high w become quite missing. Should the authors give some interpretation? It is not observed in cycle 12 though (panel e).*

Such an effect is just due to under-sampling. In a pool of 10^n oligomers, any sequence with a given ω with P(omega) < 10E-n will have a vanishing probability to appear in that sample. At cycle 12 the overall number of sequenced strands is larger than at cycle 24, due to the growing presence of PCR by-products. Thus, the right tail of the cyan distribution at the last cycle is sampled with less accuracy than at cycle 12. We have added a sentence in the revised manuscript (p5 lines 177-178) to clarify this point.

> *1. It would be interesting to further explore if another type of selection resource is used, for example protein that binds to particular sequences, i.e. transcription factors. Previous studies have used a large amount of sequence-specific transcription factors to run SELELX. Since the data have existed there, why not explore?*

This is an interesting suggestion: can we use data from “ordinary” SELEX favoring specific sequences to explore sequence evolution? Two limitations make us a bit skeptical on this path: first, the consensus sequences of DNA-binding proteins are rather short and typically target dsDNA rather than ssDNA; second, the free energy of interaction is known only for the consensus sequence but not for sequences with all possible mutations with respect to the consensus sequence, making very hard to develop any molecular understanding of the process.

> *Minor:*

1. *There is no figure legend or in-text citation of Figure 2b.*

1. *Please correct "-C" with "{degree sign}C" in lines 470, 471, 472, 477 et al.*

1. *Typos and grammar issues should be corrected. Examples are shown below (but not limited to these only):*

    - *mixed use of past and present tense.*
    - *Line 152, "basis" should be "bases".*
    - *Line 277, "a impediment" should be "an impediment"*
    - *Line 278, "a major deadly threats" should be "major deadly threats"*
      :
      We are sorry for the mistakes, and we have corrected them. Many thanks to the reviewer!